3

ELECTRON GUN TECHNOLOGY

William Clark

Hughes Research Laboratories

3011 Malibu Canyon Road

Malibu, CA 90265

December 1976

DDC

JAN 6 1977

C

REPORT DOCUMENTATION PAGE		READ INSTRUCTIONS BEFORE COMPLETING FORM
1. REPORT NUMBER	2. GOVT ACCESSION NO.	3. RECIPIENT'S CATALOG NUMBER
4. TITLE (and Subtitle) ELECTRON GUN TECHNOLOGY		5. TYPE OF REPORT & PERIOD COVERED Final Report 1 May 1972-30 Sept. 1976 6. PERFORMING ORG. REPORT NUMBER
7. AUTHOR(s) William M. Clark, Jr. and Gilmore S. Dunning		8. CONTRACT OR GRANT NUMBER(s) N00014-72-C-0496, ARPA
9. PERFORMING ORGANIZATION NAME AND ADDRESS Hughes Research Laboratories 3011 Malibu Canyon Road Malibu, CA 90265		10. PROGRAM ELEMENT, PROJECT, TASK AREA & WORK UNIT NUMBERS Program Code No. 6E20 ARPA Order No. 1807
11. CONTROLLING OFFICE NAME AND ADDRESS Office of Naval Research 800 North Quincy Street Arlington, VA 22217		12. REPORT DATE 20 December 1976 13. NUMBER OF PAGES 95 p.
14. MONITORING AGENCY NAME & ADDRESS(if different from Controlling Office) Defense Advanced Research Projects Agcy. 1400 Wilson Blvd. Arlington, VA		15. SECURITY CLASS (of this report) UNCLASSIFIED 15a. DECLASSIFICATION DOWNGRADING SCHEDULE

16. DISTRIBUTION STATEMENT (of this Report)

17. DISTRIBUTION STATEMENT (of the abstract entered in Block 20, if different from Report)

Approved for Public Release, Distribution Unlimited

18. SUPPLEMENTARY NOTES

19. KEY WORDS (Continue on reverse side if necessary and identify by block number)

Cold cathode, electron gun, e-beam pumped laser.

20. ABSTRACT (Continue on reverse side if necessary and identify by block number)

This report describes the development of two different cold-cathode, gas-filled electron guns for application to e-beam pumped gas lasers. Both e-guns, the plasma cathode electron gun and the ion plasma electron gun, were invented and patended by Hughes Aircraft Company prior to their development on this program.

SEE BACK FOR ABSTRACT

DD FORM 1473 EDITION OF 1 NOV 65 IS OBSOLETE

The first gun developed was the plasma cathode electron gun. The electron source in this device is a plasma generated within a low-voltage, hollow-cathode discharge: a thermionic emitter is not required. Electrons extracted from the plasma pass through a triode-type control grid structure and are accelerated to high energies in a plasma-free region prior to emerging from the gun through a thin foil window. The device, which is capable of both pulsed and cw operation, is characterized by durability, low cost, low power consumption, small size, and fast turn-on in comparison to thermionic e-guns. The operating characteristics of the plasma cathode e-gun as determined on this program include:

- Beam aperture   Up to 625 cm^2 demonstrated on this program. Subsequently, a cw plasma cathode e-gun with a 1000 cm^2 aperture was built

- Beam voltage   Up to 160 kV

- Beam current density   400 $\mu A/cm^2$ for up to 15 min and 1 mA/cm^2 for shorter periods operated cw; up to 60 mA/cm^2 operated pulsed

- Beam uniformity $\pm 5\%$ over beam aperture except for a 5 cm fall-off region at the ends.

Most recent efforts on the program have been directed to developing the ion plasma electron gun. Potential advantages for this gun include high-voltage operation (>400 kV), high output current density (5 to 10 A/cm^2 pulsed), pulsed and cw operation, monoenergetic e-beam, dc high voltage power supply for repetitively pulsed operation, and no control electronics floating at high voltage. In this gun, a low-pressure, thin-wire discharge produces ions which are accelerated to collide with the cathode. Secondary electrons are emitted at the cathode and are accelerated by the same high voltage and extracted through a foil window. Experimental results with a 4 cm x 40 cm aperture test device have demonstrated the concept of the ion plasma e-gun to obtain

Beam voltage   Up to 130 kV

Beam current density   2 A/cm^2 (pulsed)

Pulse widths   5 μsec (FWHM) to 150 msec.

These operating parameters are not maximum values for the gun, but were limited by the circuit constraints of the experimental arrangement.

TABLE OF CONTENTS

LIST OF ILLUSTRATIONS

5

6

I. INTRODUCTION

The program objective was to develop various nonthermionic electron guns (e-guns) and to demonstrate that they have properties suitable for application to e-beam conditioned lasers. For molecular ir lasers, an e-beam sustained system requires an e-beam energy of ≈ 160 keV with a current density of ≈ 1 mA/cm^2 (cw) and ≈ 100 mA/cm^2 (pulsed). Visible and uv excimer lasers require a pulsed e-beam with an energy >300 keV and a current density >5 A/cm^2. For these laser systems, a thermionic e-gun is normally used for molecular ir lasers and a cold-cathode field emission type gun is used for the pulsed visible and uv excimer lasers.

On this program, two different gas-filled cold-cathode e-guns were developed as replacements for the thermionic gun or the field emission gun. The first of these, the plasma cathode electron gun, was conceived as an attractive alternate to the thermionic gun. In it the source of the electrons is a low-voltage hollow-cathode discharge from which the e-beam is extracted through a partially transparent grid which serves as the anode for the discharge. During this program, the plasma cathode e-gun was developed far enough that guns have been built and used successfully to pump large-scale cw, e-beam sustained CO_2 lasers. As a result of this program, a plasma cathode e-gun was constructed (on the MIT/LRPA program) with a 1000 cm^2 beam aperture; with it we have obtained 15 min cw operation at 150 kV and current density as high as 0.4 mA/cm^2. Higher cw current densities (up to 1 mA/cm^2) were obtained with other guns for which the power supply and the foil cooling capacities were sufficient.

For cw applications to e-beam sustained laser systems, the plasma cathode e-gun has several attractive features:

- Relative insensitivity to contamination Compared to the thermionic e-gun, the plasma cathode gun does not poison if suddenly subjected to high pressures during operation. This makes both breaking the gun in and repairing it (should foil ruptures occur) much simpler.

9

- **Simpler, more compact construction**
  Thermionic guns are two to three times larger
  than plasma cathode guns of the same beam
  area. Delicate heater structures are not
  required.

- **Fast turn on**   Whereas the thermionic e-
  gun requires a warm-up period before the
  gun can be operated, the plasma cathode
  e-gun can be started and run immediately:
  the hollow cathode discharge ignites in less
  than 1 μsec.

- **Monoenergetic electron energy distribution**
  A retarding Faraday probe was used to mea-
  sure the electron energy distribution of a
  small portion of the output of a plasma cathode
  e-gun. The measured energy spread was less
  than 1.4%, the resolution limit of the experiment.

Preliminary experimental results were obtained on the contract
program; after its end, additional experimental data and the theoreti-
cal model were obtained on company IR&D funds. Development of the
ion plasma electron gun was recently begun. This gun has compelling
advantages over both thermionic and field emission guns. In the ion
plasma e-gun, a low-pressure, low-voltage thin-wire discharge is
struck at the anode (ground potential). Some ions from this discharge
accelerate to high voltage (up to 400 kV), collide with a solid cathode,
and produce secondary electrons. These electrons are accelerated back
to the anode, where they are extracted as the output e-beam. The ion
plasma gun has been operated cw and pulsed (2 to 5 μsec FWHM), at
beam voltages up to 130 kV (limit of the power supply) and at pulsed
current densities of 2 A/cm^2. Based on these preliminary experiments,
the ion plasma e-gun appears to have promise as a high-voltage, high
current density pulsed e-gun for use with visible and uv excimer laser
systems. For such an application, the ion plasma e-gun has the follow-
ing characteristics and strong advantages:

- **High-voltage operation**   Because the ion plasma
  e-gun can operate with a helium gas pressure
  below 10 mTorr, a beam voltage in excess of
  400 kV may be anticipated.

10

- **High current density** A current density between 5 and 10 A/cm^2 may be estimated for a beam voltage of 400 kV.

- **Monoenergetic beam** The energy spread of the output e-beam is determined by the energy spread of the secondary electrons emitted at the cathode. This spread is expected to be ≤0.05% at large beam voltages. Low-energy electrons resulting from the rise and fall of the supply voltage (the high voltage is dc) are not present with the ion plasma gun: they are present with cold-cathode field-emission guns.

- **Long pulse length** There is no plasma closure effect with the ion plasma e-gun. Continuous operation has been demonstrated.

- **Gun control with electronics at ground potential** The ion plasma gun is controlled by the thin-wire plasma discharge, which is run about 400 V higher than the gun's ground electrode (anode). The electronics needed to operate the gun are not required to float at high voltage, as is necessary with the plasma cathode gun and the thermionic e-gun.

- **DC high-voltage supply for repetitively pulsed operation** DC high voltage represents a strong systems advantage over the Marx-bank driven cold cathode guns in which the high voltage is pulsed.

Section II of this report will present the details of the development program for the plasma cathode electron gun. It will include a discussion of the theory of operation,[2] the construction of two large-scale guns (a 4 cm x 40 cm gun and a 5 cm x 125 cm gun), and the experimental results of extensive tests on these guns. Section II contains the results of about 80% of the time spent on the program. It includes some duplication of and a summary of the semiannual reports issued on this program for the various periods extending through August, 1975. Similarly, Section III will present the theory, experimental results, and the conclusions gained on the operation of the ion plasma e-gun. Section IV will summarize the overall results of the program.

11

II.   THE PLASMA CATHODE ELECTRON GUN

A.   Technical Description

The plasma cathode e-gun, shown schematically in Figure 1, consists of three major regions: (1) the plasma generation region, in which the beam electrons originate; (2) the extraction and control region, where electrons are removed from the plasma and transported in a controlled manner into the acceleration region; and (3) the high-voltage acceleration region, where the electrons are accelerated (without making collisions) to high energies before passing through a thin metal foil window and into the laser medium. These regions are comparable to the thermionic cathode, control grid, and the grid-to-anode space of a conventional vacuum triode.

1975-14R4
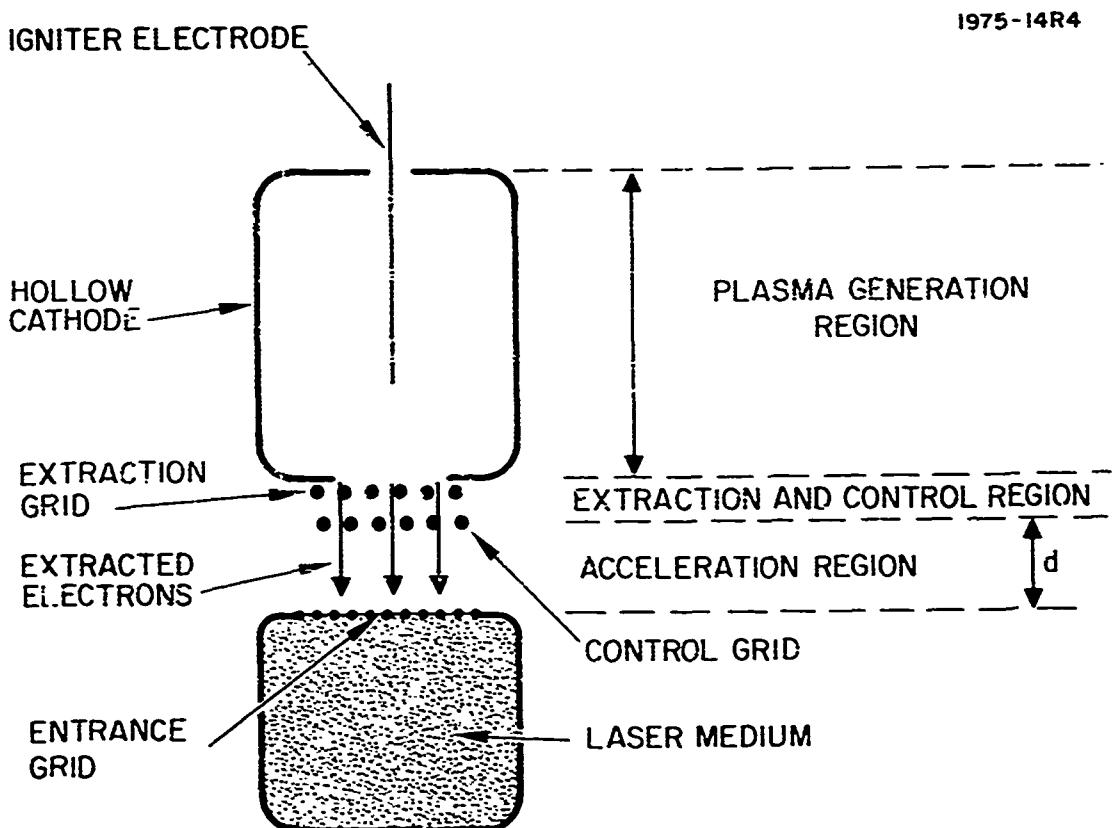
Figure 1. Schematic of the plasma cathode e-gun.

13

The plasma generation region in the present device consists of a hollow-cathode discharge struck between the hollow-cathode surfaces and the anode grid, G1. This type of discharge was chosen for its stability, reliability, simplicity, and ability to operate at the low gas pressures required to preclude gas breakdown in the acceleration region. In the present application, the discharge typically operates at a voltage of 500 to 800 V and helium pressures in the range of 15 to 30 mTorr. Helium is used because He^+ ions have relatively low sputtering yields and because it has desirable high-voltage breakdown characteristics.

The major characteristic of the hollow-cathode discharge is that most of the plasma volume is surrounded by the cathode surface. The discharge is operated in a regime where the rate of ion generation by ionization in the discharge volume is sufficient to maintain the plasma potential at, or slightly above, anode potential. Under these conditions, the discharge is a cold-cathode glow discharge sustained by secondary electron emission due to ion bombardment of the cathode surface. The applied discharge voltage V appears entirely across the cathode sheath. This has two effects: (1) ions from the plasma are accelerated by the full discharge voltage through the cathode sheath, thus gaining the energy required for secondary electron emission, and (2) the secondary electrons emitted at the cathode are accelerated through the cathode sheath to the full discharge voltage, thus acquiring an energy at which the ionization cross section for gas atoms is nearly maximum.

Maintaining a high ratio of cathode area to anode area leads to two known results. First, most ions (generated by the secondary electrons) are accelerated through the cathode sheath, intercepted by the surrounding cathode surfaces, and used with maximum efficiency for secondary electron emission, thus minimizing the rate of ion generation required per emitted electron. Second, for gas pressures where the electron ionization mean-free path exceeds the dimensions of the discharge chamber, the secondary electrons accelerated through the cathode sheath are not lost after their first transit through the discharge

chamber. Most of them are repeatedly reflected from opposing cathode surfaces and have a high probability of making ionizing collisions before reaching the anode. The discharge is thus sustained at low pressures, where the electron ionization mean-free path exceeds the dimensions of the hollow cathode discharge region.

There is a minimum pressure below which this mode of discharge cannot be sustained. This is believed to be due to the following circumstances: as gas pressure is reduced, the number of oscillations which a secondary electron must perform before making an ionizing collision increases. As the number of oscillations increases, the probability for an oscillating electron to fall on the anode before making an ionizing collision increases; its probability of being captured rather than reflected by a cathode surface also increases.[1] Both effects reduce the percentage of oscillating electrons which are effectively used in making ionizing collisions. As the utilization efficiency of the oscillating electrons decreases with decreasing gas pressure, the energy which must be imparted to them to maintain the required rate of ion generation increases; this leads to the experimentally observed increase of discharge voltage with decreasing gas pressure. As the discharge voltage increases with decreasing gas pressure, the ionization collision cross section for the oscillating electrons decreases, and eventually the rate of ion generation per emitted secondary electron becomes smaller than the corresponding rate of ion loss. The gas pressure at which this happens is the minimum below which this discharge mode cannot be sustained.

Electrons are extracted from the discharge plasma through anode grid G1 and pass through the control grid G2 into the accleration region. Voltages of typically 0 to -100 V relative to G1 may be applied to G2 to control beam intensity. Grid G2 also provides isolation between the low-voltage glow discharge region and the high-voltage acceleration region. Alternately, it is possible to control beam current by varying the hollow-cathode discharge current through the potential of G1.

15

The width d of the acceleration region is critical to the successful operation of the plasma cathode electron gun, since the entire electron acceleration voltage is applied across this gas-filled gap. To produce a high-energy electron beam with a narrow energy distribution, the number of inelastic collisions which the electrons make with gas molecules in this region must be kept to a minimum. This can be done by operating at low gas pressures and maintaining a small acceleration region width, thus avoiding the formation of a gas discharge in this region. At typical operating pressures (15 to 40 mTorr), the mean free path for 100 keV electrons with gas atoms is ≈ 100 m^2. To meet this requirement, the width is determined primarily by the principles of vacuum breakdown. Experience has shown that parallel-plate electrodes will, conservatively, withstand applied fields of 70 kV/cm without breakdown in vacuum.[3] This result is not changed if gas, at sufficiently low pressures, is present in the interelectrode space. The vacuum breakdown voltage V is plotted as a function of d in Figure 2.*

Increasing the gas pressure increases the probability of gas or Paschen breakdown. The present device operates to the left of the Paschen minimum, as shown in Figure 2, for a helium pressure of 50 mTorr. As is well known, the Paschen breakdown voltage depends on the product pd and, therefore, a reducing pressure will proportionally increase the width d for which breakdown would occur at a given voltage.[4] It has been experimentally demonstrated under the present program that, as expected, the Paschen breakdown characteristic is unaffected by the presence of an electron beam in the acceleration region.

As seen from Figure 2, there is a region between the two breakdown characteristics where high-voltage operation is possible without incurring breakdown. In the present device, d is chosen for a given maximum operating voltage (150 kV for this example) so that the operating point will lie nearer to vacuum breakdown characteristics. This is

_____

*There exists a wide scatter in data for vacuum breakdown as well as for Paschen breakdown in helium. The curves shown in Figure 2 represent a conservative interpretation of this data, supplemented by our own measurements.

16

2179-14R1
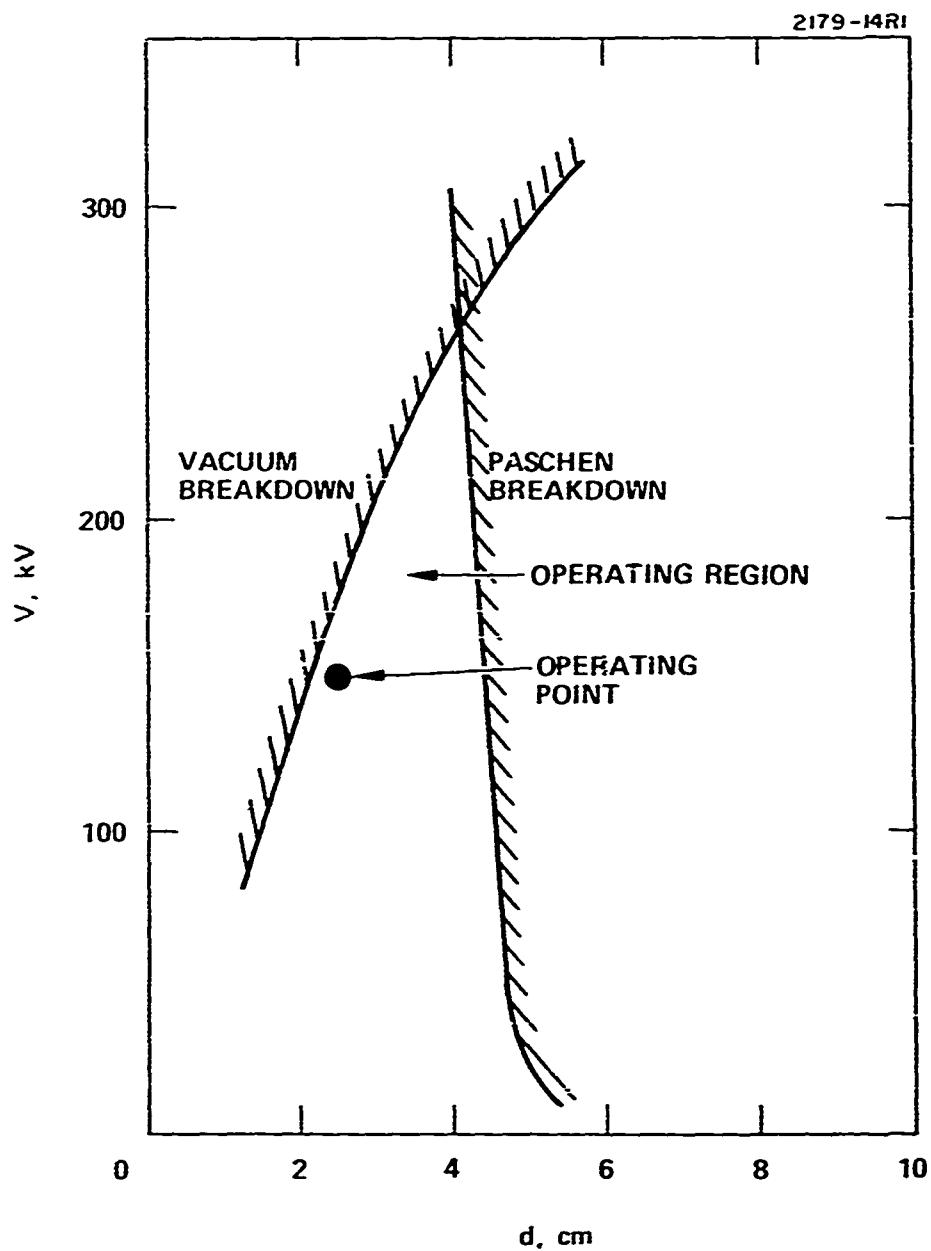
Figure 2. Low-pressure breakdown voltage in the plasma cathode accelerating region as a function of gap width. The Paschen curve is for a pressure of 50 mTorr of helium.

17

desirable since this characteristic is expected to be more stable in time than the Paschen curve, which is sensitive to the presence of out-gassing products. Figure 2 also shows that at lower gas pressures a plasma cathode gun may be designed for operation with beam voltages in excess of 200 kV.

Figure 3 summarizes the voltage and current requirements for the plasma cathode e-gun; this is based on data obtained under typical pulsed and cw operating conditions. The current level of $2 I_B$ supplied by the high-voltage source assumes a transmission of 50% for the foil window assembly. Measurements on existing plasma cathode devices indicate that the discharge anode current is about equal to the beam current incident on the foil window structure. Therefore, the discharge power supply also operates at $2 I_B$ in either the pulsed or cw mode, depending on the desired application. As shown, the control grid oper-ates at a slightly negative potential relative to the anode and collects a current of ~15% of the extracted current. The igniter, which provides the background ionization to permit initiation of the hollow cathode dis-charge without requiring excessive voltages, operates cw at typically 10 mA and 300 V.

The plasma cathode electron can be operated cw or pulsed. Essential operating characteristics are the same for both modes when the average discharge and beam currents in pulsed operation are com-parable to the dc levels in cw operation. The maximum cw or average discharge current allowable is determined by the heat absorbing and dissipating characteristics of the hollow cathode surfaces and the anode grid structure. The maximum beam current density is set by the allowable heat loading by the beam in the foil window.

B.   Specific Electron Gun Designs

Initial experiments testing the plasma electron gun concept were performed using a rectangular geometry gun having a 3 cm x 10 cm aperture and operated in the pulsed mode. These tests were success-fully completed; they demonstrated scalability to large-area e-beams with a 15 cm x 10 cm aperture gun which had a rectangular electrode geom-etry similar to that of the 2 cm x 10 cm gun mentioned above.

18
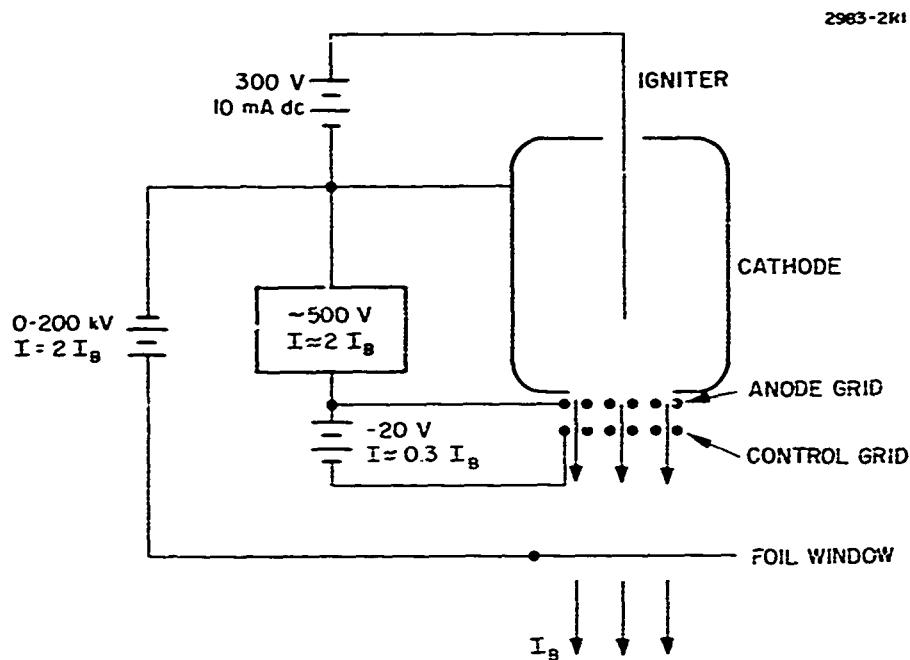
Figure 3. Plasma cathode power supply schematic.

Applying the plasma cathode e-gun to pump lasers required designing a gun with a cylindrical electrode geometry which incorporated a more compact high-voltage feedthrough. Two cylindrical geometry guns with rectangular e-beam apertures of 4 cm x 40 cm and 5 cm x 125 cm were constructed and tested on this program. The design of these guns and of the coaxial high-voltage feedthrough is described in this section.

1.   Rectangular Geometry Plasma Cathode E-Guns

The device which was used to evaluate the plasma cathode e-gun concept is shown in Figure 4. The hollow cathode was formed from stainless steel and had inside dimensions of 3.6 cm x 13.7 cm x 5.9 cm deep. Two igniter electrodes (not shown) protruded into the discharge volume from the upstream cathode surface. The grid structure (G1 and G2) consisted of two identical 44% transparent stainless-steel meshes spaced 0.8 cm apart. The hollow cathode and grid assembly were mounted in the end of a reentrant electrode which protruded into the cylindrical ceramic standoff. This standoff also served

19

as part of the vacuum enclosure. The collector electrode was
reentrant from the opposite end of the ceramic cylinder and spaced
2.5 cm from the opposing electrode. With this device, the character-
istics of beam extraction and acceleration could be studied without
involving the complicating factors of foil transmission. In the experi-
mental studies. the cathode was grounded and the collector was biased
at up to 150 kV. Suitable corona shields were fitted to the exterior of
the device and the assembly was mounted on an LN_2 trapped oil diffu-
sion pump station. The system was first evacuated. then filled with
helium. and finally gettered to remove outgassing products. During
the experimental program. various probes were mounted as part of
the collector to permit measuring beam current density distribution,
energy distribution, and foil transmission characteristics of the beam.
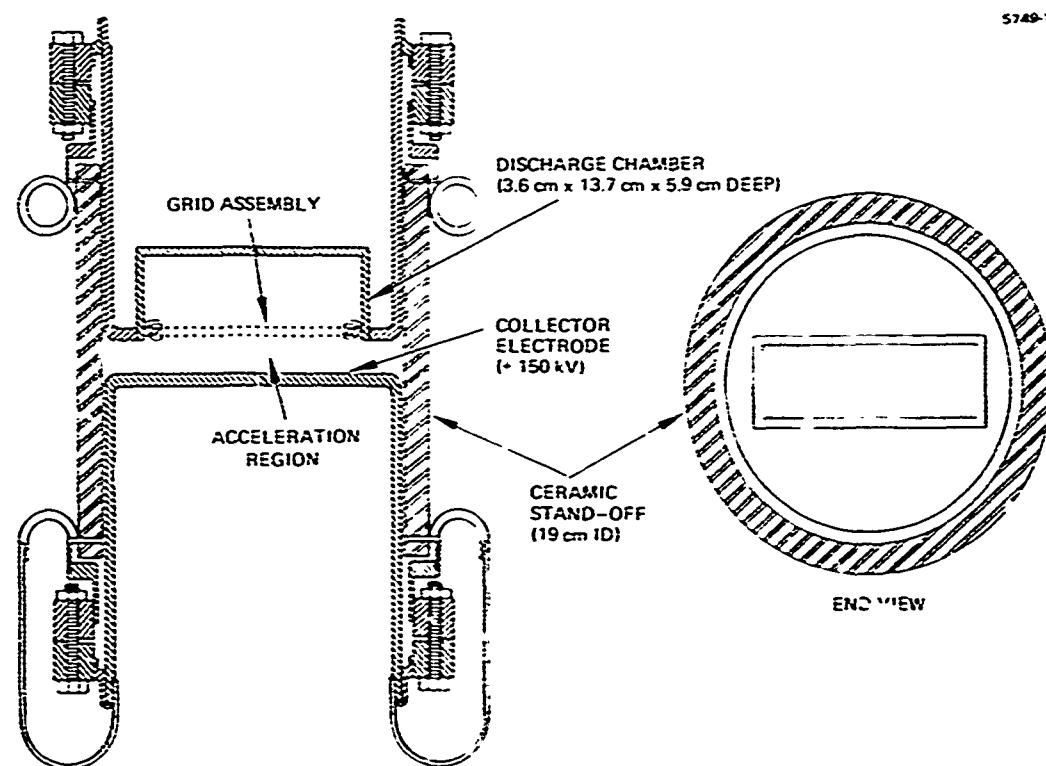
Figure 4. Experimental apparatus used to evaluate small plasma
cathode e-gun devices.

A larger version of the same gun design was built and tested to show scalability of the plasma cathode e-gun to a beam aperture of 5 cm x 10 cm. Its dimensions were 12.5 cm x 17.5 cm x 5 cm deep for the stainless-steel hollow cathode and 3.5 cm for the acceleration region (collector electrode to opposing control grid). Apart from these dimensions and the fact that six (instead of two) igniter wires were placed in the hollow cathode to initiate the discharge, the two guns were essentially identical.

2.   Coaxial, Compact High-Voltage Feedthrough

The high-voltage insulator design required for application to the plasma cathode e-gun must satisfy rather specialized requirements. In addition to the usual constraints imposed by vacuum and dielectric breakdown, there are also constraints due to Paschen breakdown. For operation at high voltage (<150 kV), the insulator was designed to (1) have the high voltage completely enclosed by grounded surfaces to eliminate flash-overs in air and improve safety, (2) be small and lightweight, (3) use a moderate-sized ceramic, and (4) adapt to most e-gun sizes without redesign.

As a result of these constraints, large ceramic paths were not possible and, based upon the design criteria given by Schonhuber,[5] the metal-ceramic-vacuum interfaces should be shielded from the high electric field region. In the design used, the 4 cm gap between the electrodes in the gun or the test device (4 cm was chosen to allow reliable 200 kV operation) is carred close to the outer surface of the ceramic, and the electrode surfaces are folded back along the ceramic. Best results were obtained with a 2 mm gap between the i.d. of the electrodes and the o.d. of the ceramic and with a 5 mm radius of curvature at the electrode edge. The ceramic chosen was alumina, Al-300.

The resulting design is shown in Figures 5 and 6 in a test vehicle configuration. High voltage is supplied to the inner structure by a coaxial cable which is connected within a field shaping structure containing pressurized SF_6. The 4 cm gap between the inner and outer
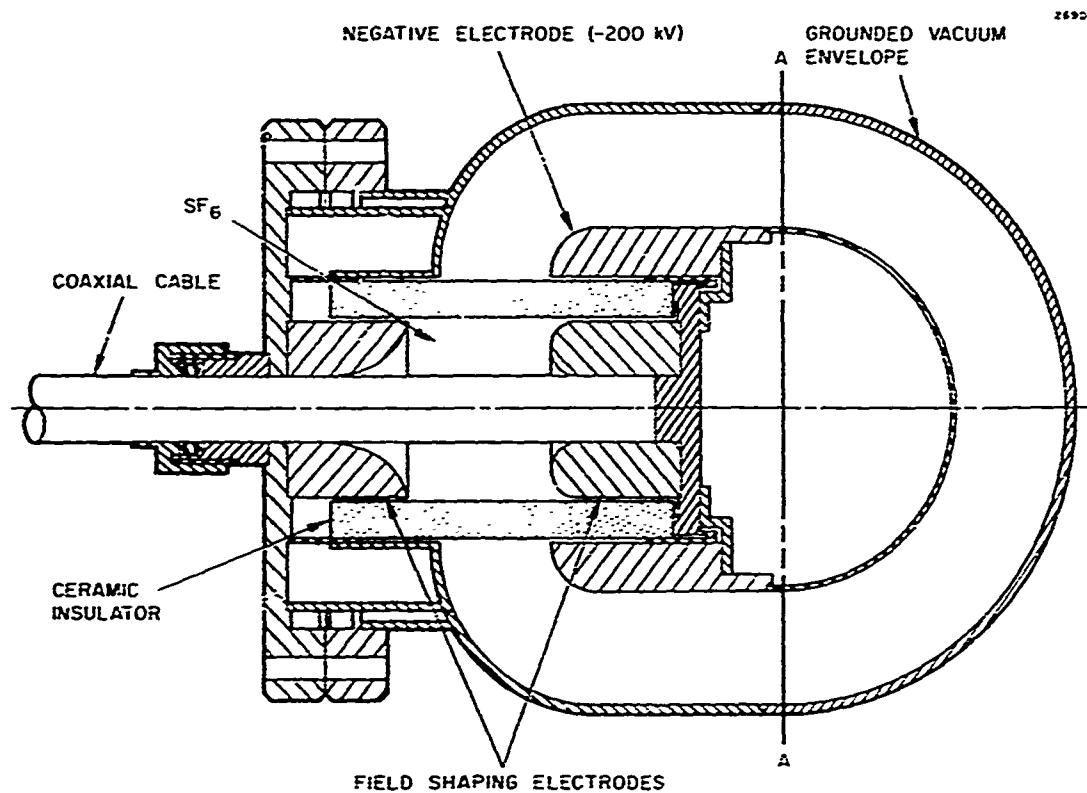
Figure 5. High-voltage feedthrough test vehicle.
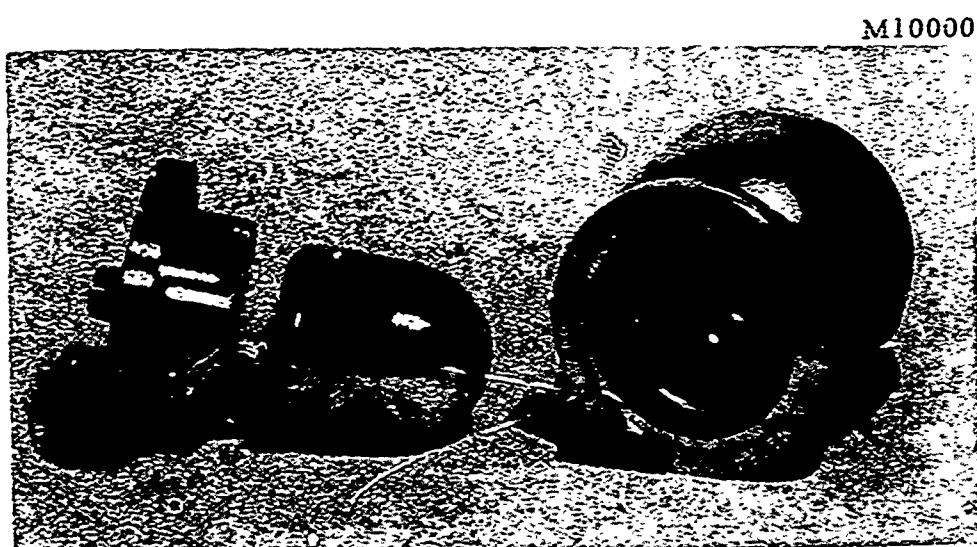
Figure 6. Disassembled high-voltage feedthrough test vehicle.

22

structures is equivalent to the plasma cathode e-gun acceleration region. Applied to a e-gun, in this design there would be a separation at plane A-A, (see Figure 5) and the hollow cathode electrode structure would be inserted. In the test configuration, the feedthrough was subjected to voltages up to 200 kV (the limit of the power supply) and current, gas pressure (both in the high-voltage gap and the SF_6 in the feedthrough chamber), and X-ray emissions were monitored. After stable, quiet operation was attained at the high voltage limit for 5 min, the Paschen breakdown characteristic of the device was determined. The results (shown in Figure 7) are consistent with the results of similar experiments with the various guns tested. Finally, 200 kV was applied across the electrode structure with a helium pressure of 56 Torr, and throughout the 5 min experiment the leakage current was less than 3 μA.

When used with an e-gun, the electrical power for the cathode, anode grid, control grid, and igniter electrode must be supplied by the feedthrough. For this purpose, a 2.3 cm diameter coaxial cable was passed through the center of the ceramic tube to a four-pin connector located within the innermost field shaping electrode. The center conductor of this cable is a copper tube which facilitates routing the four conductors to the connector. The copper tube carries current to the cylindrical discharge cathode. The field shaping electrodes within the ceramic tube are designed so that the electric field lines merge smoothly from the 4-cm gap into the coaxial cable. SF_6 at 50 psig inhibits breakdown within the ceramic tube. A 3 to 5 kV spark gap is provided between each grid and the cathode can. This limits the voltage differences between components and electrical leads should an arc strike to the grid structure.

3.   Design of the 4 cm x 40 cm E-Gun

Applying the plasma cathode e-gun concept to pump e-gun lasers required developing a cylindrical geometry gun in which the longitudinal dimension of the gun could be easily increased to match the required length of the laser to be pumped. Before constructing a gun with this geometry, we first developed the following two design concepts:

23
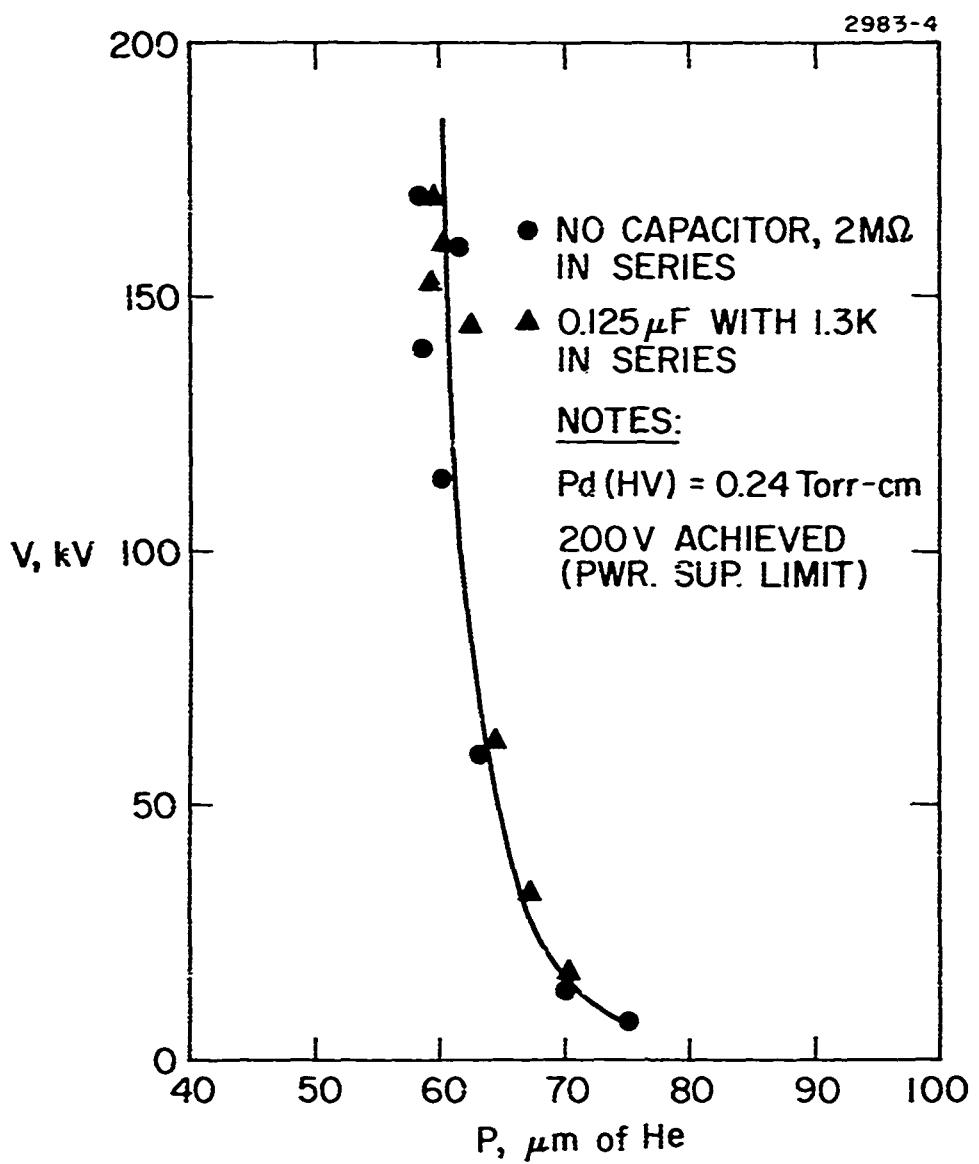
Figure 7. High-voltage feedthrough test results (Paschen curve).

- The coaxial, compact high-voltage feedthrough as described above.

- The demonstration that a stable hollow-cathode discharge could be maintained in a long (40 cm) cylindrical cavity.

After these tasks were successfully completed, the first coaxial cylindrical plasma cathode e-gun, with a 4 cm x 40 cm beam aperture, was built. Figure 8 shows a cross-sectional schematic of the basic coaxial gun design; Figure 9 illustrates the layout of the e-gun. Figure 10 is a photograph of the two major e-gun components: the inner cylinder (which contains the hollow cathode discharge) and the outer grounded cylinder (which contains the thin foil window and support and which also serves as the vacuum envelope).

The hollow-cathode discharge chamber is formed by the 12 cm i.d. inner stainless-steel cylinder. Once ignited, the hollow-cathode discharge runs at a voltage, typically around 500 V, which is largely insensitive to the discharge current. The operating voltage depends on the helium gas pressure and the presence of contaminants.

The beam extraction and control region consists of the anode grid, G1, and the control grid, G2. Both grids are formed from a screen of square stainless-steel mesh having a 0.014 cm wire diameter and a transmission of 52%. The screen is spot-welded onto a 0.09 cm thick piece of perforated stainless steel with 0.4 cm diameter holes on 0.48 cm centers. The perforated metal backing for the screen is used for support and to define the plane of the grid. The control grid is located 0.8 cm from the anode grid: when operated at a negative voltage relative to the anode of 0 to 100 V, the extracted beam may be varied from its maximum value to near cutoff. Grid G2 also serves to provide isolation between the low-voltage hollow-cathode discharge and the high-voltage acceleration region. The beam current may also be controlled by varying the hollow-cathode discharge current through the potential of G1.

The anode grid (G1) design is dependent on the desired operating mode. For high current pulsed operation, the anode Debye sheath

25
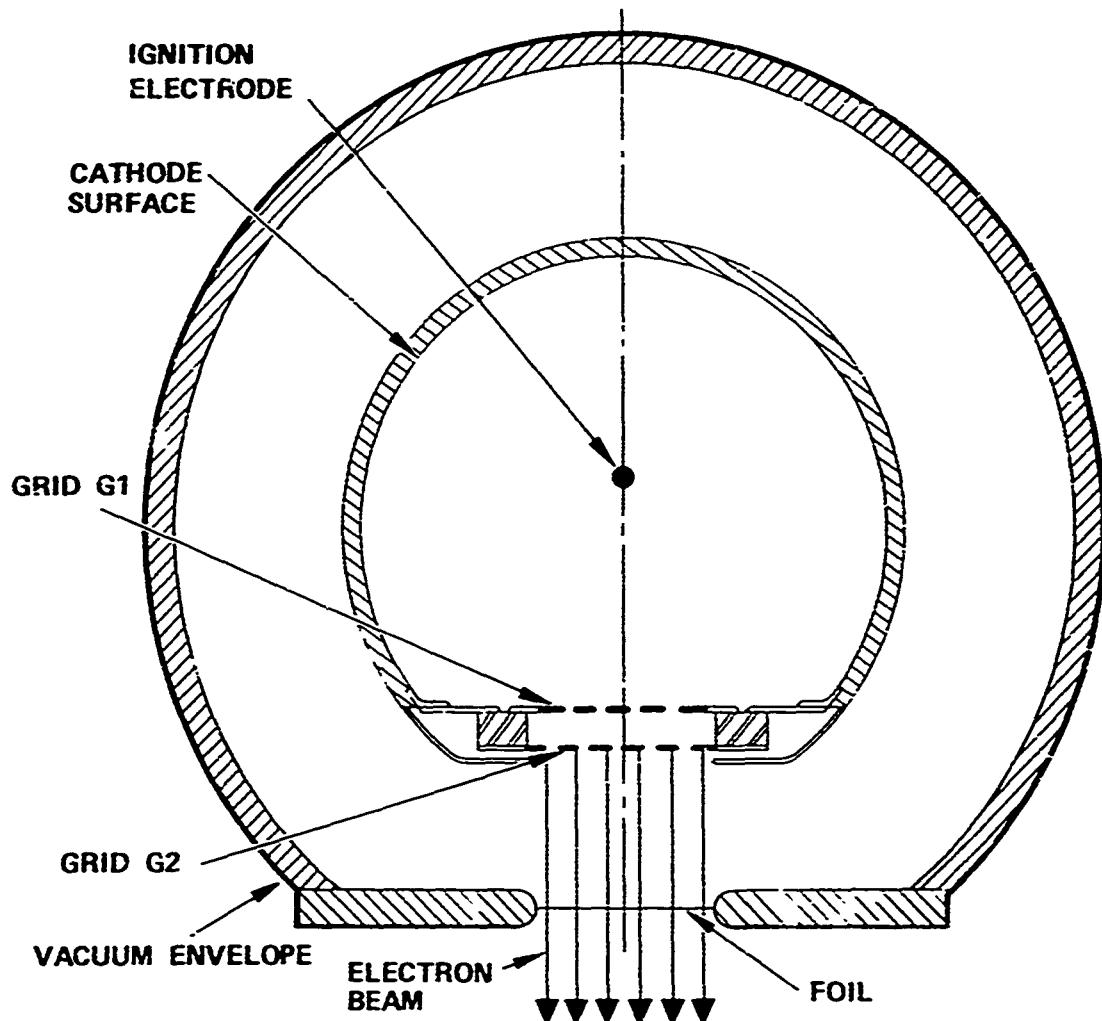
Figure 8. Cross section of the coaxial e-gun design.

0.2083-6

HOLLOW CATHODE
DISCHARGE CHAMBER

ACCELERATION
REGION

FOIL WINDOW
FLANGE

HIGH-VOLTAGE FEEDTHROUGH
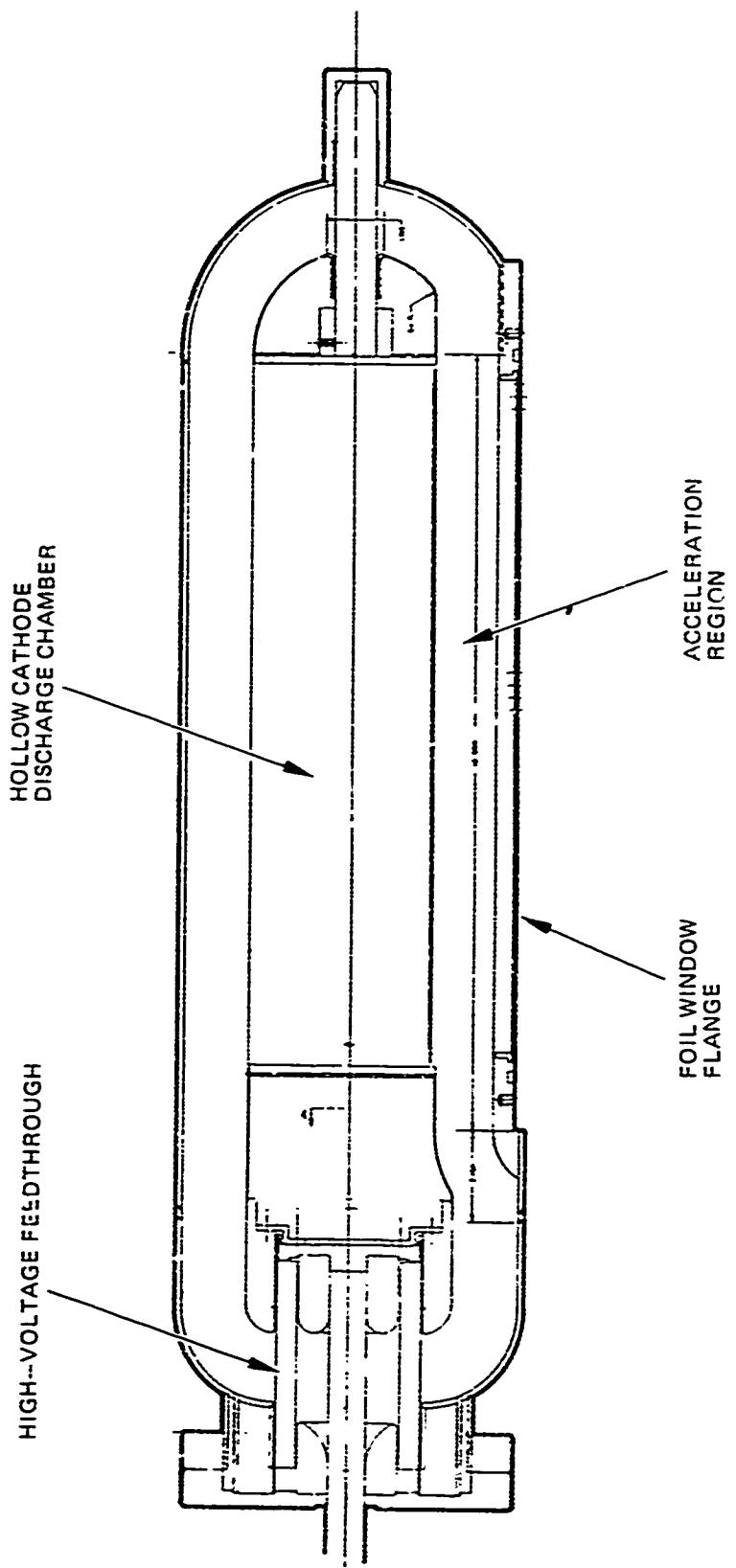
Figure 9. High-energy 4 cm by 40 cm e-gun.

27
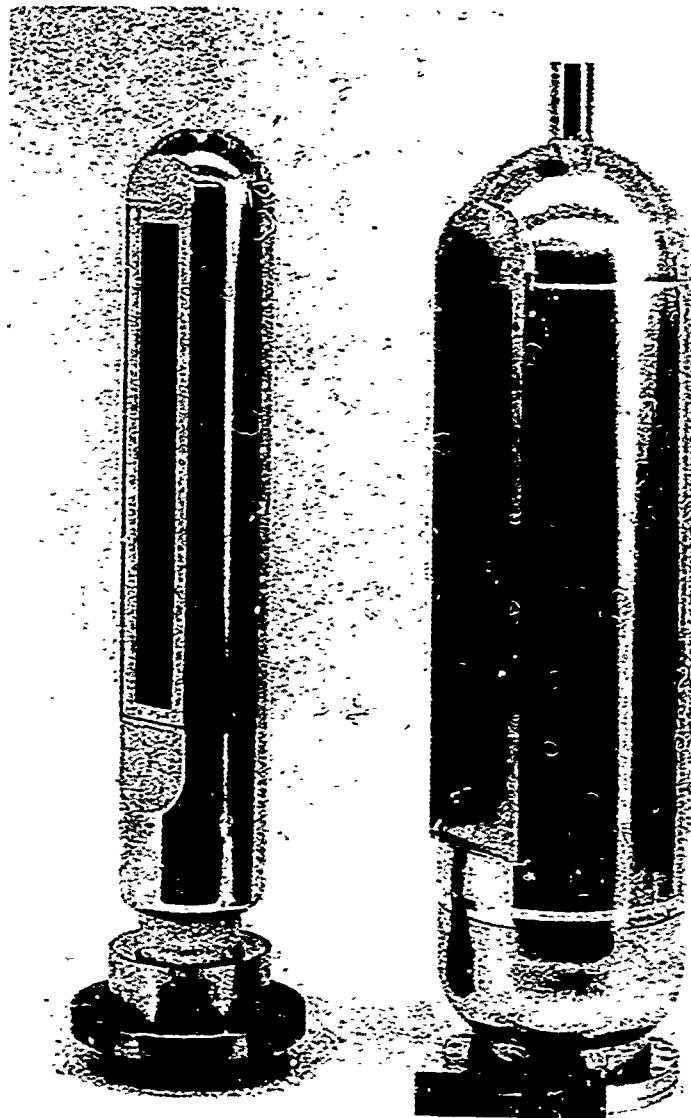
Figure 10.   Inner and outer cylinders of high-voltage
4 cm x 40 cm e-gun.

thickness is typically 0.1 mm and the cathode Langmuir sheath thickness is about 2 mm. In this case, the dimensions of the sheath discontinuity, where anode and cathode potential surfaces meet, is on the order of a few millimeters, which is much less than the beam width. Also, the anode surface need only extend over the dimensions of the beam to provide good beam uniformity. This also results in a minimal anode area, which is desirable for maintaining a low discharge voltage and a high ratio of beam current to anode current.

Discharge current and, therefore, plasma density are generally much lower for cw operation. This results in the formation of anode and cathode sheaths with thicknesses of about 1 mm and 1 cm, respectively. Therefore, the region of sheath discontinuity, which can lead to nonuniform anode current densities, extends over a distance of about 1 cm. It is desirable in this case to provide a 1 cm wide nontransparent extension at the periphery of the anode grid (see Figure 8) to remove the sheath discontinuity from the area of beam extraction. In the present case, the grid mesh is mounted on a stainless-steel frame which provides the desired 1 cm wide border and also serves as a sputter shield for the ceramic pieces which support and separate the two grids.

A 0.025 cm diameter tungsten igniter electrode initiates the large-volume cold-cathode discharge. Experiments indicate that this electrode should extend the full length of the hollow-cathode discharge to maintain good plasma uniformity. This would presumably result from enhanced coupling between various discharge regions due to currents flowing in the electrode. This ignition electrode, which operates at a current of about 10 mA, is biased by a 1000 V dc power supply connected with a 50 k resistor in series. We do not expect the definition of any of these values to be critical.

The inner and outer cylinders (refer to Figures 8 and 9) are contoured so that an approximate 4 cm spacing is maintained at all points between the two cylinders. This spacing is chosen assuming a 200 kV operating voltage. With reference to Figure 2, a smaller gap would result in larger field strengths, which could cause vacuum

29

breakdown. A larger gap would reduce the gas pressure range for which operation would be possible. This spacing is maintained with field shaping electrodes. Electrodes are provided which extend the plane of the control grid, G2, smoothly into the cylindrical cathode surface. There are also contoured electrodes, located at each end of both the inner and outer cylinders, to minimize electric field concentrations. All parts of both cylinders are formed from nonmagnetic 304 stainless steel electropolished to minimize sharp surface protrusions.

The surface of the cylindrical vacuum envelope is mated with the flat window support flange, as shown in Figures 8, 9, and 10. A wire mesh "high-voltage anode" is provided between the thin foil window and the acceleration region to maintain the 4 cm acceleration region width and to avoid focusing the electron beam. This wire mesh greatly reduces the potential gradient in the region between it and the foil window, thereby reducing the contribution of ions produced in this region, and of electrons reflected from the foil, to gas breakdown processes. Such a potential defining plane will always be necessary since it is desirable to: (1) locate the foil window close to the laser medium and (2) provide substantial flange thickness so that it will not distort due to the pressure difference across the vacuum chamber wall.

For high average beam current guns, the design of this high-voltage anode grid is strongly influenced by its (1) thermal properties, (2) electrostatic focusing, (3) electrostatic field enhancement, (4) effect on Paschen breakdown, and (5) beam interception. (This will be discussed in detail for the 5 cm x 125-cm e-gun.) In the present design, a 78% transparent square molybdenum mesh formed from 0.0125 cm diameter wires has been used. Radiation cooling of this mesh permits it to withstand high input power densities without melting.

A solid Al-300 alumina post is used to provide mechanical support of one end of the inner cylinder. The electrode design in this region is similar to that used at the ceramic o.d. of the high-voltage feedthrough.

The foil window vacuum seal is made with an ungreased Type 747 Viton O-ring. All components used within the e-gun are of good vacuum quality.

4.   Large-Scale Electron Gun (5 cm x 125 cm Apertures

A large-scale e-gun, with a full-size aperture as required to pump a high-power CO_2 laser, Peacemaker, was designed and built on this program. The design of this gun was completed after initial testing on the 4 cm x 40 cm e-gun had been completed, providing confidence of the performance of the basic cylindrical electrode structure gun. As a result, the 5 cm x 125 cm e-gun is similar in design to the 4 cm x 40 cm gun; it has the following specific requirements:

- Beam energy, 150 to 175 keV

- Average beam current density, 0.1 to 0.5 mA/cm^2

- Minimum operating time, 5 sec

- Half angle of beam convergence at foil windows, ~10°.

Beam convergence was chosen to help compensate for the divergence of the beam at the edges due to scattering by the foil window. The value 10° was chosen to be convenient to design with a 5 cm wide beam and cylindrical electrode geometry.

Figures 11 and 12 show the design layout of the 5 cm x 125 cm plasma cathode e-gun. The main difference between the 4 cm x 40 cm and 5 cm x 125 cm guns is that the latter has a curved anode-control grid structure to provide the necessary focusing.

The cathode is made from a 304 stainless-steel (nonmagnetic 304, 315, or 321 stainless steel is used for all parts unless stated otherwise) cylinder of approximately 18 cm i.d. The grid system is supported by brackets attached to this cylinder. The anode and cathode grids have curvatures of approximately 12 and 11 cm, respectively,

31

3820-3
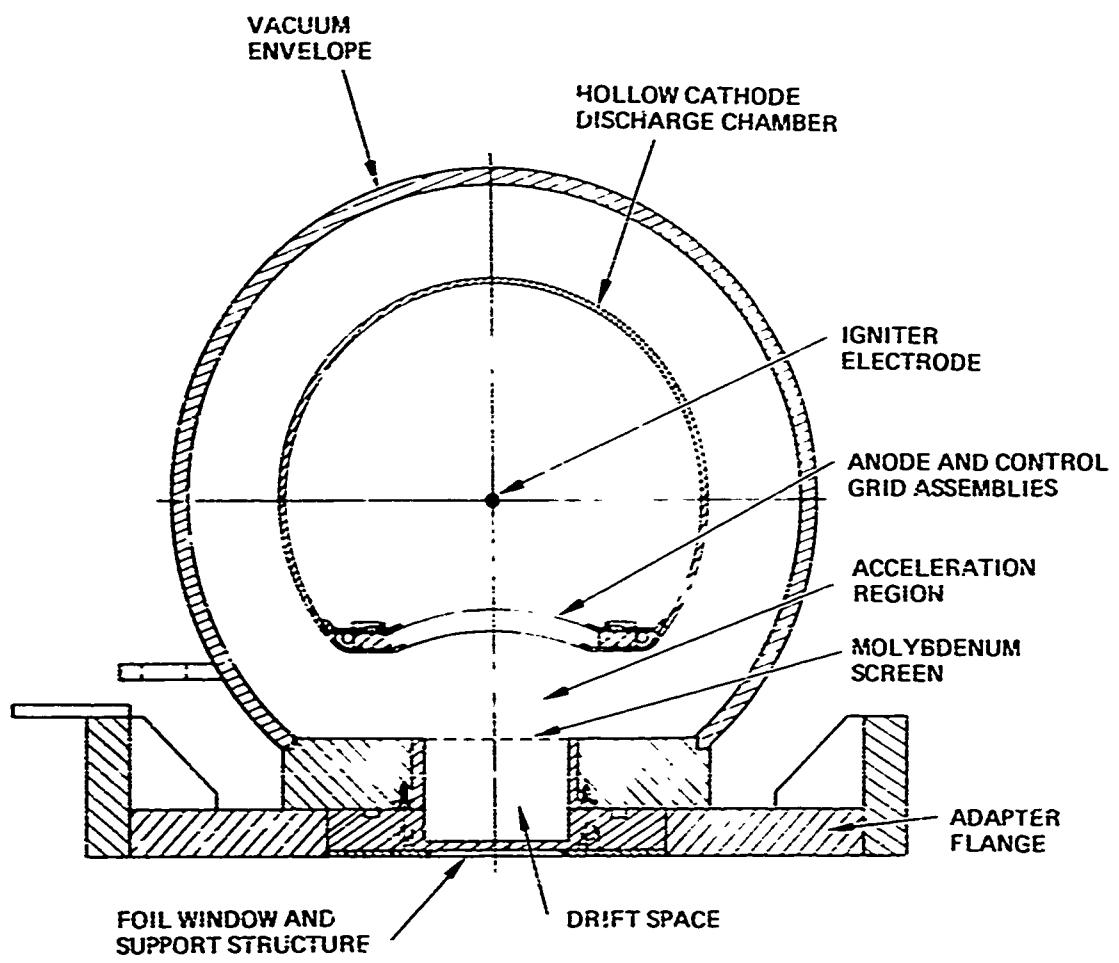
Figure 11. Cross section of 5 cm by 125 cm plasma cathode e-gun.

32

3820-1

HOLLOW CATHODE
DISCHARGE CHAMBER

PUMP PORT

CERAMIC
SUPPORT

ANODE AND CONTROL
GRID ASSEMBLIES

HIGH-VOLTAGE FEEDTHROUGH

HIGH-VOLTAGE INSULATOR

GAS INLET
PORT
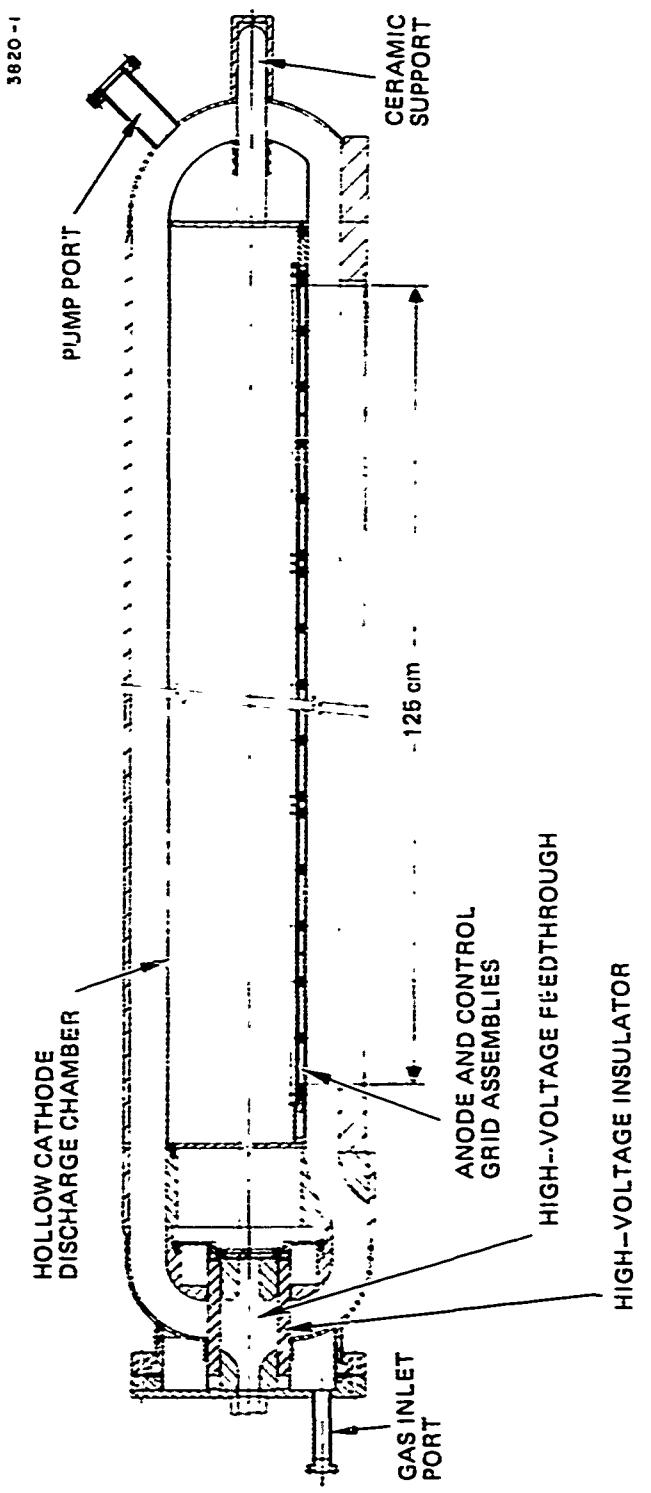
-125 cm -

Figure 12. Layout of 5 cm x 125 cm plasma cathode e-gun.

and are spaced 0.8 cm apart. The grids, which are formed from perforated stainless-steel sheet stock 0.095-cm thick with 0.4-cm diameter holes and a transmission of 63%, are covered with 59% transparent stainless-steel wire mesh. The perforated material provides mechanical support; the fine mesh, for which the wire spacing of approximately 0.05 cm is less than the Debye sheath thickness, defines the plasma boundary. The supporting ceramic pieces are shielded, as in the 4 cm x 40 cm device, to prevent deposition of sputtered material. A metal tube used to route electrical leads is included within this shielding.

The spacing between the inner and outer cylinders is maintained at close to 4 cm, which results in an e-gun o.d. of 27 cm. In the grid region, this spacing varies from 3.6 cm to 4.5 cm due to grid curvature. After acceleration, the electrons pass through a potential-defining molybdenum mesh (78% transparent) and into a drift region 4.5 cm long. This drift region is needed to locate the foil window near the lasing medium. The thin foil window is supported against the external atmospheric pressure by a 75% transparent aluminum bar structure (see Figure 13). As shown in Figure 11, a flange is provided which adapts the gun to the laser. The grids, foil support, and flange are designed such that the major support ribs do not shadow the e-beam. Figure 14 shows the completed inner cylinder and the vacuum envelope. The foil support structure and the e-gun adapter flange are not present in this photograph.

M10340
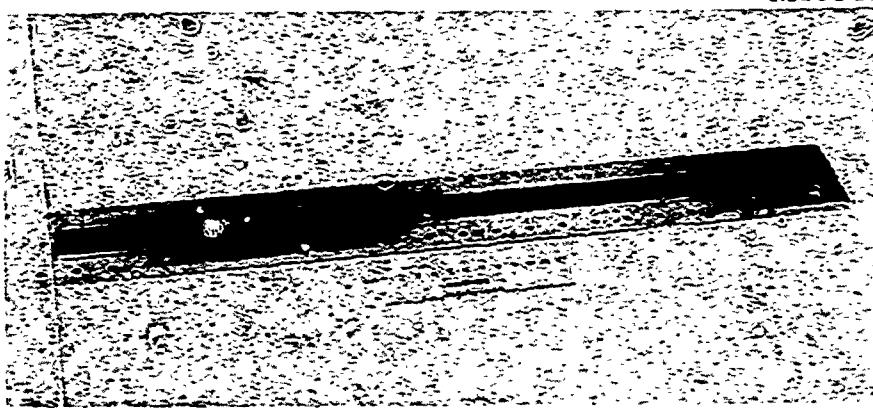
Figure 13. Foil support structure.

34

Figure 14.   Inner and outer cylinders of 5 cm x 125 cm
e-gun.

The high-voltage feedthrough, ceramic support post, and field shaping electrode structures have designs similar to those of the 4 cm x 40 cm e-gun. In the present device, due to the somewhat larger gun diameter, the maximum electrical field strengths are 20 to 50% lower than in the 4 cm x 40 cm device.

In the design shown in Figure 11, the beam width and convergence angle at the foil window are related to the overall cross-sectional dimensions of the discharge chamber through the desired ratio between anode and cathode areas. This ratio should be about six, based on experimental results with the 4 cm x 40 cm gun for operation at 30 to 50 mTorr of helium and the required beam extraction. Therefore, as convergence angle and/or extracted beam width are increased, the anode width and discharge chamber diameter must increase. Furthermore, as the convergence angle increases, the variation in distance increases between the curved control grid and the flat high-voltage acceleration electrode. This variation in the fields in the acceleration can be compensated for by also curving the molybdenum electrode; however, this complicates the design. We evaluated several designs with differing grid curvatures with the aid of a digital computer program. This program provided the potential distribution within the acceleration region and the resultant electron trajectories. The final design chosen was the one which most closely satisfied the above design criteria. From these considerations, the present design was selected to maintain the spacing between the inner and outer electrode potential surfaces at 4 cm ±10%.

Figure 15 shows the dependence of convergence angle at the foil window on distance from the center of the window, calculated for the present design. The curve's peak is associated with the curvature reversal at the edges of the control grid, which is necessary to minimize electric field concentrations. The beam edge is chosen as the peak of this curve, which gives a beam width of 4.2 cm and a convergence angle of 9.4°.

36
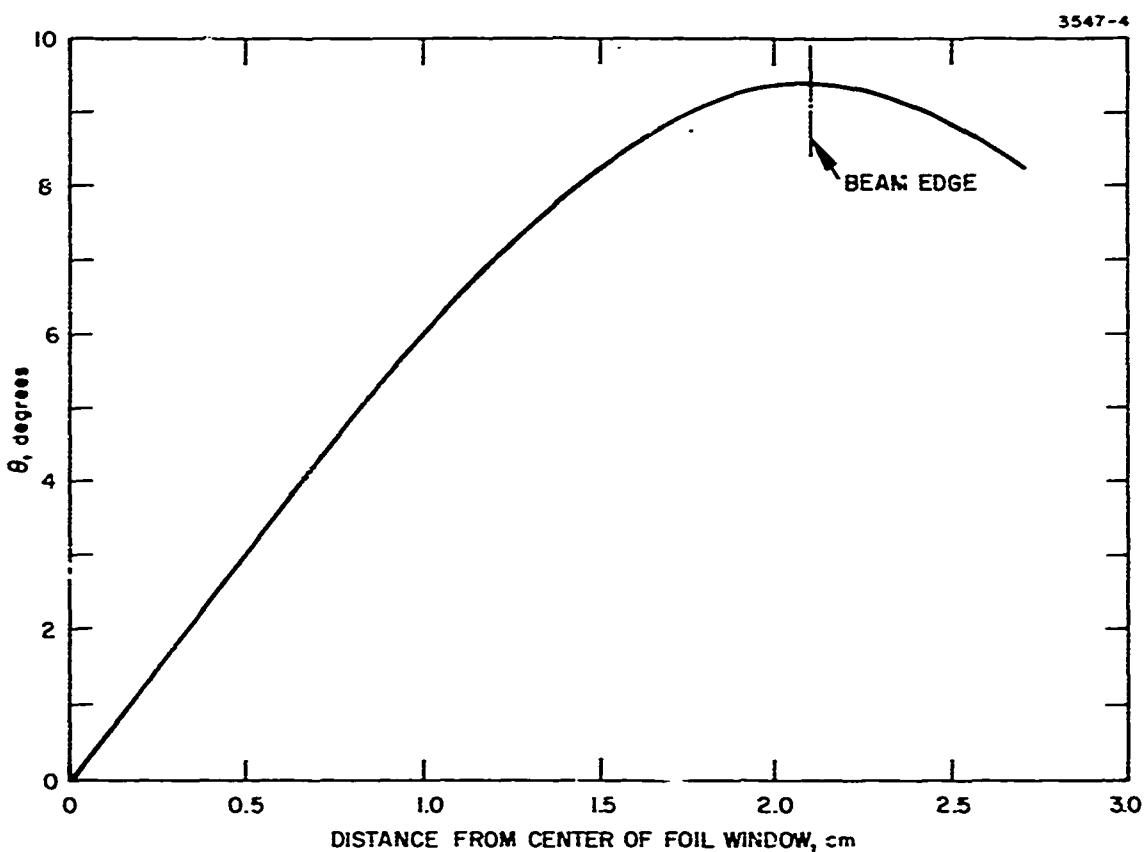
Figure 15. Dependence of beam convergence angle at the foil window on the distance from the center of the beam.

Figure 16 shows the effect of focusing on the transverse beam current density distribution assuming a uniform current density incident on the anode grid. Focusing leads to a 45% reduction of the beam current density at the beam edge.

The high-voltage anode grid, as discussed previously, defines an equipotential surface on the positive side of the acceleration region. This component was formed by a molybdenum mesh in both the 4 cm x 40 cm and 5 cm x 125 cm e-guns. The design of this component is influenced by its: (1) thermal properties, (2) electrostatic focusing, (3) electric field enhancement, (4) effect on Paschen breakdown, and (5) beam interception.

37
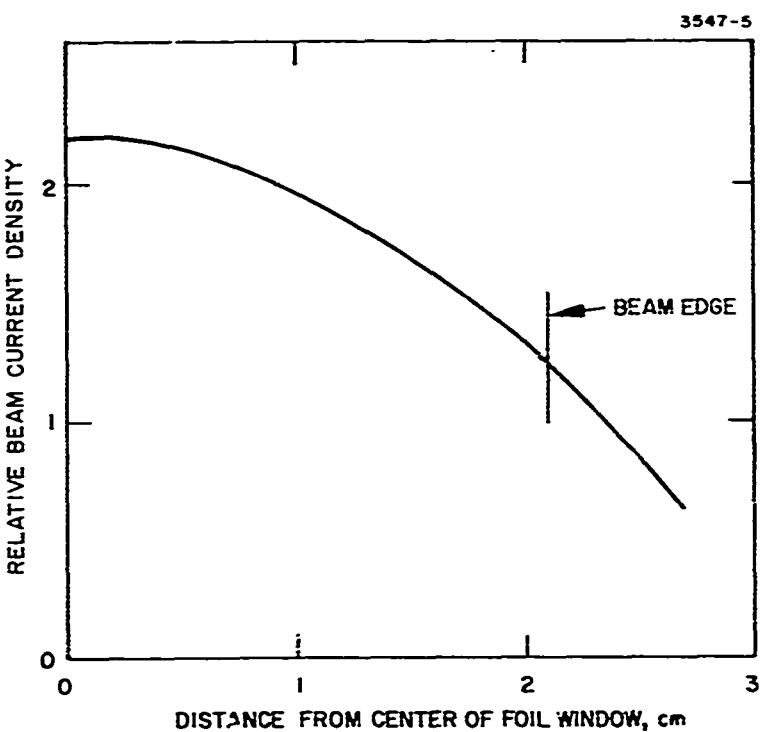
Figure 16. Dependence of beam current density on the distance from the center of the foil window.

The high-voltage anode grid is heated by direct bombardment by high-energy electrons. Cooling occurs through radiation and conduction. Simple calculations show that the maximum temperature attained when radiation cooling alone is considered is given by:

$$T_{max}(°K) = 770 \left[\frac{j_B V_B}{\epsilon (A_r/A_i)} \right]^{1/4} ,$$

where j_B is the beam current density after the foil window in amperes, V_B is the beam voltage in volts, ϵ is the emissivity of the grid, A_r is the area from which radiation takes place, and A_i is the area which intercepts the e-beam. For a molybdenum grid with square or round bars intercepting 0.5 mA/cm^2 at 175 kV, this temperature is 1900°C and the melting point is 2610°.

38

The relationship for a bar grid, which is cooled by conduction to a cold flange, is given by:

$$T_{max}(°C) = \frac{L^2}{4} \frac{j_B V_B}{k\ell} \quad ,$$

where L is the length of the bars, k is the thermal conductivity, and ℓ is the depth of the bars. For the same beam conditions as used above, this gives a temperature close to the melting point for both molybdenum and copper bars with dimensions of 6 cm long and 0.2 cm deep. Thus, radiation cooling would dominate for these conditions.

Thermal conduction can be increased by increasing the depth of the bar grid; however, defocusing the electron beam by the local potential distribution near the grid would lead to increased interception by the grid and a loss of grid transmission. It can easily be shown that the transmission of a bar grid is given approximately by

$$T = 1 - \frac{a}{A} - \frac{\ell}{2W} \quad ,$$

where a is bar width, A is the spacing between bar centers, and W are the depth and width of the acceleration region, respectively. Referring to the previous example, increasing   to 0.4 cm (in the third term in the above expression, which is due to defocusing) will result in a 5% loss in grid transmission.

Thermal expansion is an additional factor relating to thermal properties. If a rigid bar grid is used, either the gun flange will be severely stressed or the bars will distort. It may be possible to design the bars so that they will distort in a controlled manner, but this is probably difficult. Alternatively, a fine molybdenum mesh such as has been employed above can be used. Such a mesh will lose heat by radiation and will operate at a temperature well below its melting point. Thermal expansion is easily allowed for through screen distortion (macroscopic distortion does not disturb the beam since its velocity is very high near the positive electrode). Furthermore, a fine mesh will not suffer unwanted transmission losses as a result of defocusing.

It is important that the geometrical transmission of the high-voltage anode grid be high. However, as the transmission increases, so does the electric field enhancement factor at the grid wires. If this factor becomes too large, vacuum breakdown will occur. The enhancement factor, which can be easily obtained starting from the development of Spangenberg,[6] is given by:

$$\delta = 1 - e^{-\pi(1-T)^{-1}}$$

Table I illustrates how this factor depends on the grid transmission T. The average electric field strength in the acceleration region of the 5 cm x 125 cm e-gun at 175 kV is 40 kV/cm. Since it is generally desirable to maintain the field below about 70 kV/cm, the grid transmission should be between 70 and 80%. For this transmission, as determined with the 4 cm x 40 cm e-gun, there is negligible effect on the Paschen breakdown characteristics. Thus, 78% molybdenum mesh, as used with the 4 cm x 40 cm gun, is also quite suitable for the 5 cm x 125 cm e-gun.

Extensive testing and use of the 5 cm x 125 cm e-gun were not part of this program. However, the gun was operated successfully to pump the Peacemaker laser at the HAC Culver City facility. In that application, the gun was reported to have attained 150 keV beam energy with up to 0.2 mA/cm^2 average beam current density for up to a 1 sec cw run.

TABLE I. Dependence of the Electric Field-Enhancement Factor δ on Grid Transmission T

T, %	δ
70	1.7
80	2.1
90	3.7
100	∞

T1426

40

C. Experimental Results

Extensive experimental data was obtained in operating the guns just described. In this section the experimental results will be presented. Experiments with the 3 cm x 10 cm and the 10 cm x 15 cm aperture guns (with a rectangular electrode geometry and for pulsed operation only) determined the i-v characteristics of the hollow-cathode discharge and the energy spectrum of the extracted e-beam. These results have also been shown to be valid for the cylindrical guns. The cylindrical, 4 cm x 40 cm, e-gun has operated both cw and pulsed, and data on the uniformity and stability of the extracted e-beam was obtained.

1. Results Obtained with the Rectangular Geometry E-Guns

These data were obtained from a configuration in which the cathode was maintained at ground potential, the grids pulsed (positive) by means of a Velonex Model 350 pulser, and the high-voltage anode and foil or collector plate ran at (positive) high voltage. Pulse lengths of 10 to 100 μsec were obtained. Subsequent data obtained for cw operation with other guns has shown behavior similar to that of the pulsed guns for cases in which the peak pulsed current densities were 10 times the cw current density.

Figure 17 illustrates typical hollow-cathode discharge characteristics obtained in the absence of beam extraction. Figure 17(a) shows the dependence of the voltage of the anode grid V_{G1} on the grid current I_{G1} for helium pressures of 17 and 20 mTorr. For higher currents the voltage tends to saturate as expected. The dependence of V_{G1} on helium pressure is shown in Figure 17(b) for a constant discharge current. As pressure decreases, discharge voltage increases until ignition becomes unreliable. For long-life operation it is desirable to have minimal sputtering, which means that the discharge voltage should be minimized. This suggests that larger pressures are desirable. However, to ensure that Paschen breakdown does not occur in the acceleration region of the device, which operates at the same pressure as the discharge, it is desirable to minimize the helium pressure. From consideration of these competing factors, an operating pressure in the range of 15 to 30 mTorr is used.

41
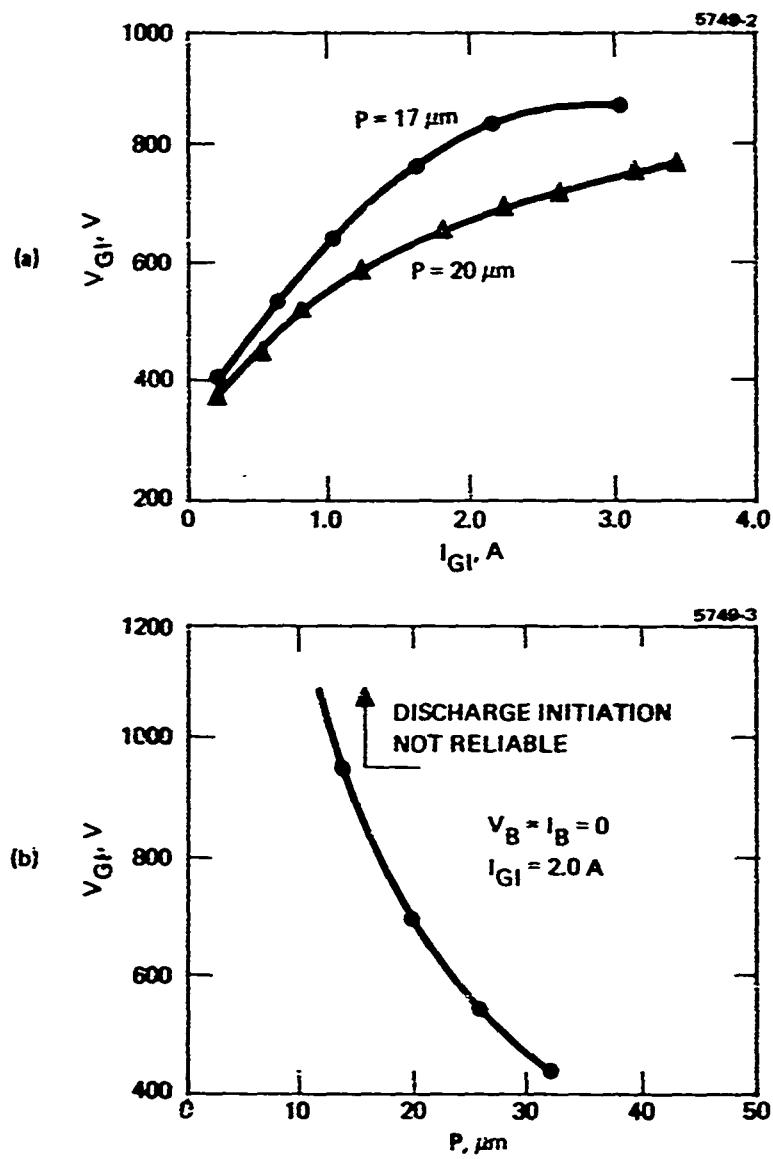
Figure 17. Hollow cathode discharge character-
istics for an anode grid area of
11 cm^2 with $I_{G2} = I_{collector} = 0$ and
$V_{G2} = V_{cathode} = V_{G1}$.

Plasma probe measurements performed using one of the two igniter electrodes as a Langmuir probe indicate that the electron temperature is in the range 4 to 10 eV and that the plasma potential is slightly more positive than the potential applied to grid G1. These results are consistent with the usual model of the hollow-cathode glow discharge.

Figure 18 illustrates the electron beam control characteristic, which is equivalent to the control characteristic of a standard vacuum triode. In this figure, the voltage across the acceleration region (between collector and cathode) is plotted as a function of $(V_{G2} - V_{G1})$ for a fixed beam current $I_B = 1.0$ A and fixed anode grid voltage V_{G1}. These data are for an 11 cm^2 beam area. As the beam voltage increases, the potential of the control grid must be made more negative to maintain a constant beam current. The slope of the linear portion of the curve gives the triode equivalent amplification factor μ, which was measured to be 6×10^3. An approximate theoretical calculation gives a value of 7.5×10^3 (Ref. 6). This agreement indicates that, as desired, no plasma exists within the acceleration region and that the control and acceleration characteristics are well understood.

$$\mu = -\frac{\delta V_B}{\delta (V_{G2} - V_{G1})}$$
$$= 6 \times 10^3 \text{ (EXPERIMENT)}$$
$$= 7.5 \times 10^3 \text{ (THEORY)}$$
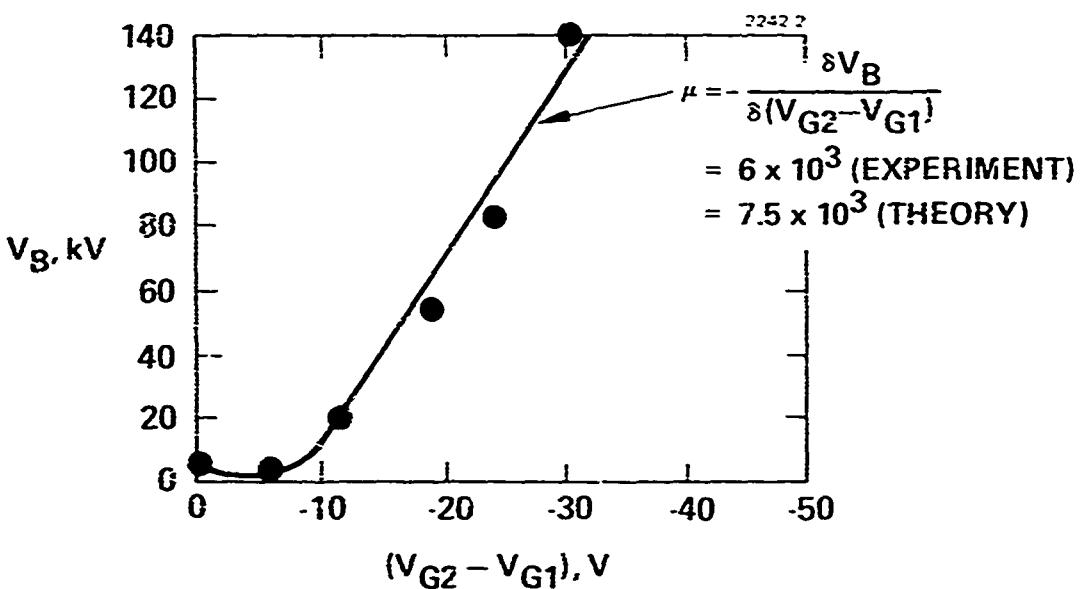
Figure 18. Electron beam control characteristics.

Figure 19 illustrates the electron beam energy distribution measured at the center of a 30 cm^2 beam. The data were obtained using a retarding Faraday probe to analyze the current passing through a 0.1 cm diameter aperture in the collector. The beam energy was 50 keV (determined by the available retarding potential power supply) and the current density was 146 mA/cm^2. The dashed portion of the curve is estimated so that the integrated current is consistent with the beam current density. Most of the beam (90%) fell in the major peak having a full-width half-maximum of 1.4 keV, which is less than 3% of the total energy. It is expected, furthermore, that most of the measured width is associated with the measuring device rather than beam properties. The small peak at low energies is also thought to be caused by instrument effects resulting from generation of electron-ion pairs within the volume of the Faraday probe. In any case, the measurements demonstrate the formation of a highly monoenergetic beam, as expected.

2.   CW Results with the 4 cm x 40 cm E-Gun

This gun was operated in a configuration in which the high-voltage anode (including the solid collector plate or the foil and foil support) was at ground, and the cathode and grids were held at negative high voltage. As a result, the anode discharge power supply, the igniter supply, and the control grid bias supply were floated at this negative high voltage. Such an arrangement is typical of a practical case in which a gun is used to pump a laser where the laser discharge region would be at ground. The high-voltage power supply used for these experiments is rated at 40 mA, so the maximum current density obtainable is limited to ≈ 0.25 mA/cm^2. Experiments with another power supply (20 kV, 200 mA) showed that the gun could operate with a current density of 1 mA/cm^2.

High voltage stand-off tests, which were performed without beam extraction, demonstrated that the present design is capable of operating at beam voltages up to 200 kV. As the voltage was initially increased, some arcing and x-ray emissions were observed; these decreased over time. The 200 kV level was achieved after 1 to 2 hours of conditioning after tube assembly.

44
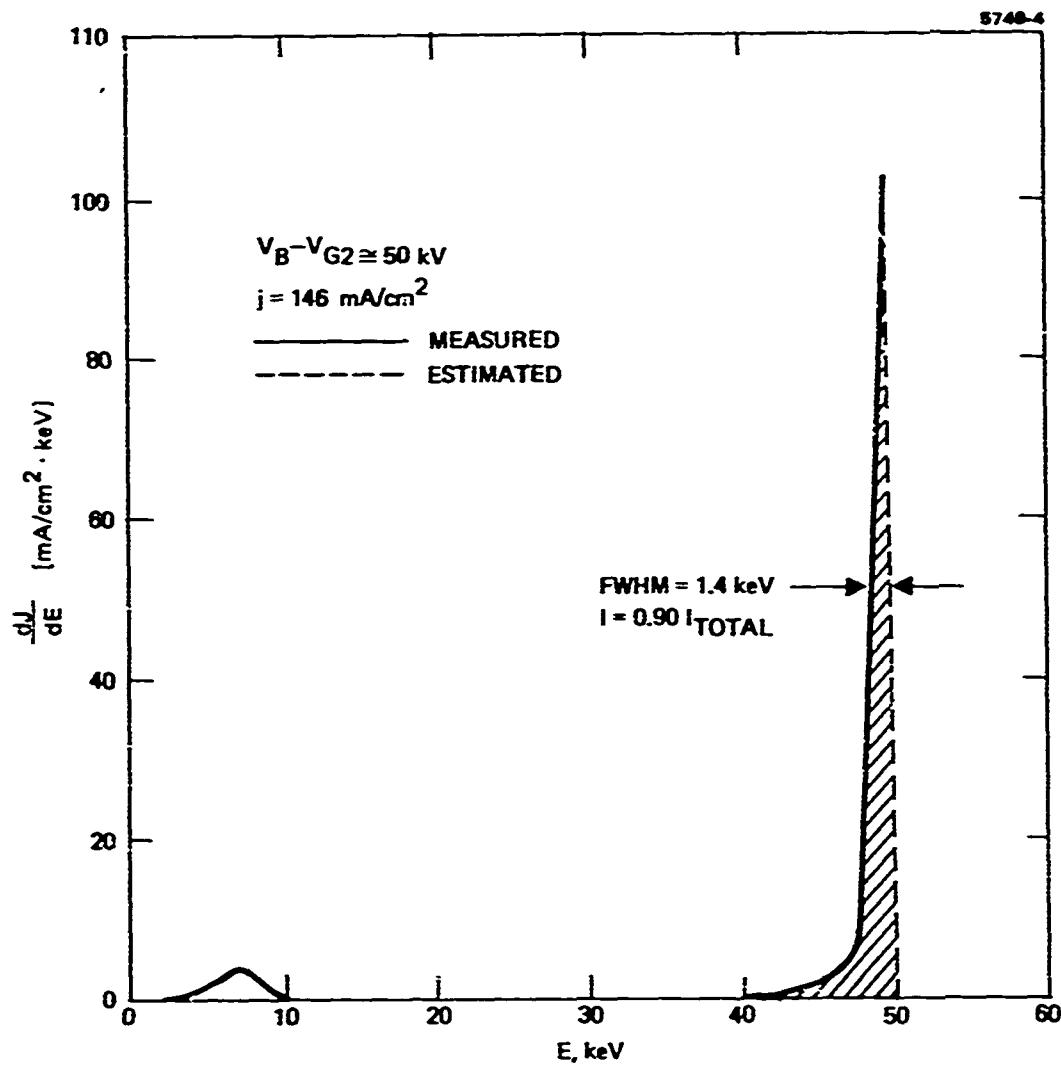
Figure 19.   Electron beam energy distribution.

a.   Data Taken with a Solid Collector Plate (No Foil) —
The e-gun characteristics with beam extraction are illustrated in
Figures 20 through 22.   Figure 21 shows that the beam current I_B is
proportional to the discharge current.   These data were obtained at a
control grid potential of -23 V (the control potential is measured rela-
tive to the anode potential) for beam energies of 50 and 100 keV.   The
small current remaining after the discharge current was reduced to
zero is due to electrons generated by the igniter.   If the anode and

45
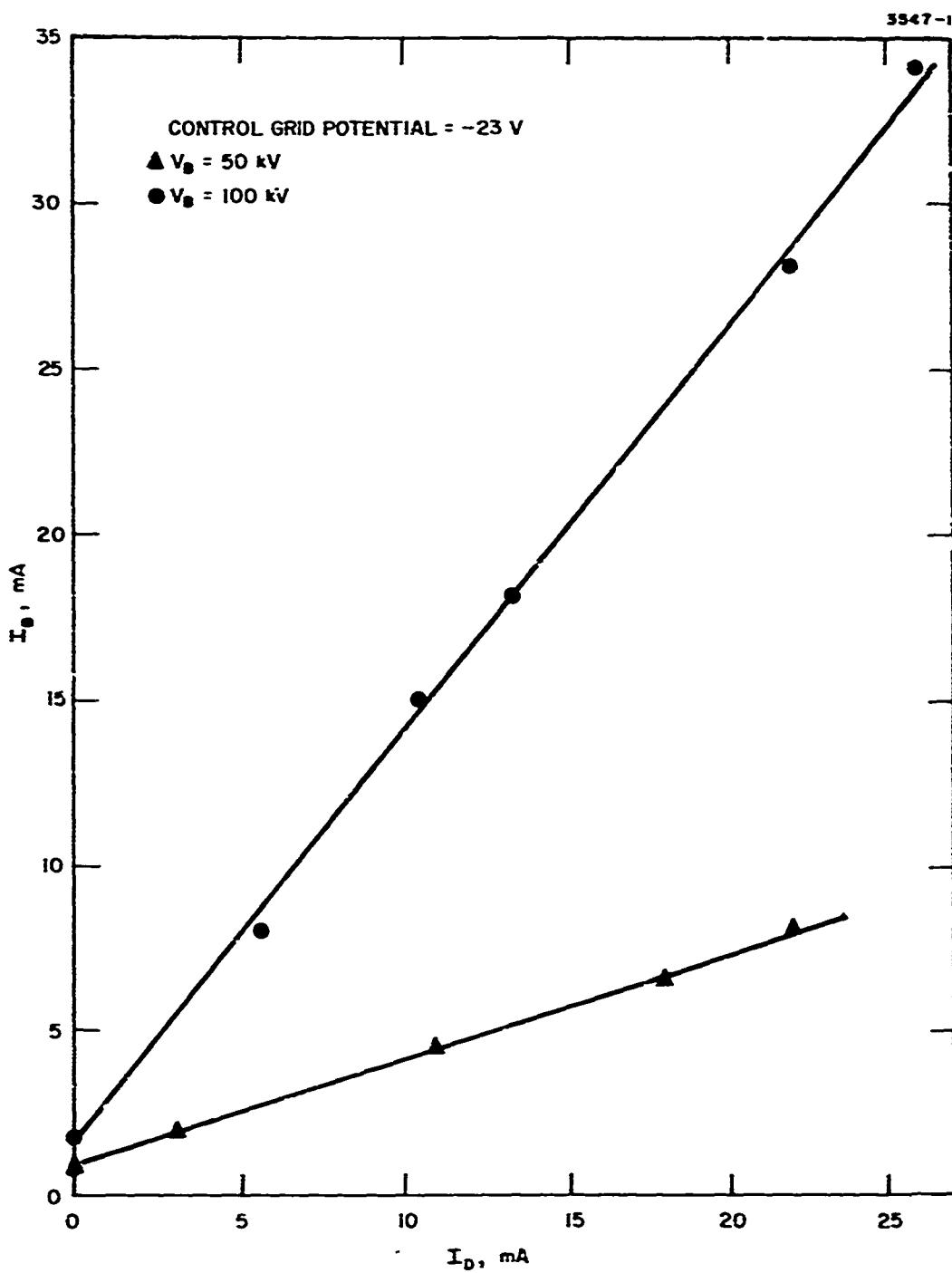
Figure 20. Dependence of the electron beam current I_B on the discharge current I_D with the beam voltage V_B as a parameter.

46

3547-2
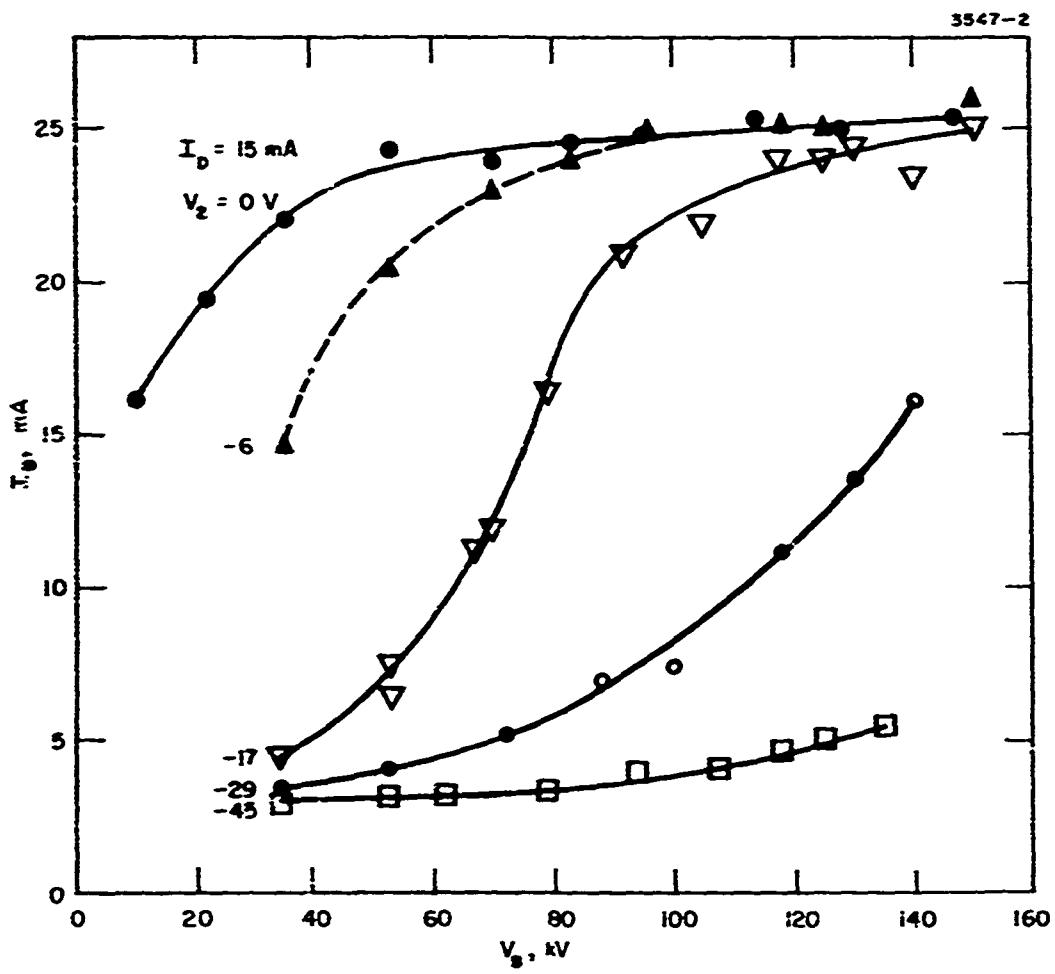
Figure 21. Dependence of beam current I_B on beam voltage V_B with the control grid potential V_2 as a parameter.

BEAM VOLTAGE, V_s = 140 kV

DISCHARGE CURRENT, I_D = 15 mA

I_s, mA

V_2, VOLTS RELATIVE TO ANODE
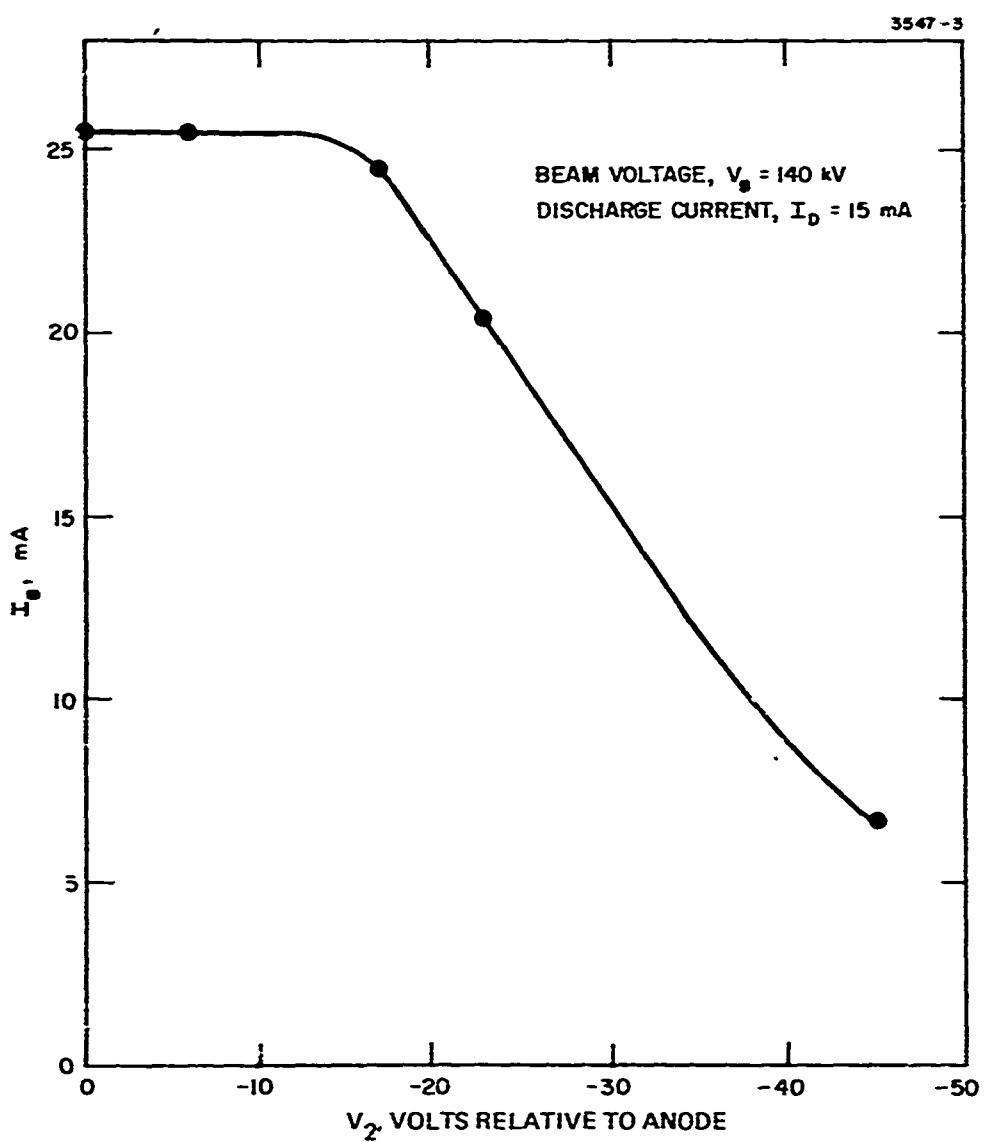
Figure 22.   Dependence of beam current on control grid potential.

control grids are connected to cathode potential, this residual beam current is reduced to 0.1 mA.

Figure 21 shows the dependence of beam current on beam voltage for various control grid potentials with discharge current fixed. It is seen that beam current saturates with beam voltage and that this saturation generally occurs at lower beam voltages as the control potential is made more positive. These data are partially replotted in Figure 22, where I_B is given as a function of the control potential V_2 for a beam voltage of 140 kV. In this figure, the saturation of I_B as V_2 becomes more positive is particularly evident.

The apparent potential of the control grid is given by

$$(V_2)_{apparent} = V_2 + \frac{V_B}{\mu} \ ,$$

where μ is the equivalent triode amplification factor.[6] This factor, which is obtained from the slope of V_B as a function of V_2 with I_B and I_D held constant, is approximately 4.3×10^3. Therefore, the departure from saturation in Figure 22 occurs for an apparent control potential about 10 V positive with respect to the anode. The reason for this characteristic is not clear. The linear dependence of beam current on discharge current indicates that space charge limitations are not important. However, the positive value of the effective control potential should preclude electron retardation. This leaves two possibilities: the hollow-cathode plasma potential is being affected by the control potential and/or a secondary plasma exists between the grids. Both of these situations are difficult to analyze on the basis of existing data.

As shown in Figure 22, I_B does not go to zero rapidly at the large negative control potentials. This is probably due to the electron energy distribution, which contains both primary electrons with $E \sim 100$ eV and plasma electrons with $E \sim 1$ to 10 eV.

The saturated value of beam current indicated in Figures 21 and 22 can be explained as follows. Electrons are only collected by "anode potential surfaces" (i.e., anode grid, control grid, and window structure), since all other surfaces are negative with respect to plasma

49

potential. Ions, however, are collected by both cathode and anode surfaces, since both are negative with respect to the plasma. Under saturation conditions, when the apparent potential of the control grid is positive relative to the anode, the ions are reflected back to the anode grid. In addition, because the secondary electron yield due to ion impact on cathode surfaces is much less than unity, the total ion current is equal to the total electron current. In other words, $j_i A_T = j_e A_{AG}$, where j_i and j_e are respectively the collected ion and electron current densities and A_T and A_{AG} are, respectively, the total and anode grid areas. Since the control grid intercepts few electrons, due to focusing of beam electrons through it, we can write: $I_B = j_e T A_{AG}$, where T is the transmission of the anode grid. The current collected by the anode can be written as: $I_A = [j_e(1 - T) - j_i] A_{AG}$. The ratio I_B / I_A at saturation is then given by:

$$\frac{I_B}{I_A} = \frac{T}{(1 - T) - \left(\dfrac{j_i}{j_e}\right)} = \frac{T}{(1 - T) - \left(\dfrac{A_{AG}}{A_A}\right)} .$$

For our case, $T \cong 0.53$ and $A_{AG} / A_A \cong 0.12$ so that $I_B / I_A \cong 1.5$. This agrees reasonably well with the experimentally indicated ratio of 1.66. In these tests, a beam current of 30 mA (0.19 mA/cm^2) was extracted from the discharge at up to 162 keV for 5 sec. Small arcs (wihtout high voltage power supply overload) occasionally occurred at this level. Such occurrences were rare at a beam energy of 150 keV and operation was quite reliable.

Electron beam stability was assessed by observing electron beam and discharge currents with Pearson current transformers and an oscilloscope. Generally, oscillations on the extracted beam were associated with ripple in the various power supplies. Since beam current is proportional to discharge current, ripple in the latter influences the former. Therefore, it is desirable to use a constant current discharge power supply to minimize ripple on the electron beam.

50

Argon and air have been added to the helium working atmosphere with no noticeable effects on stability. They do, however, reduce the maximum operating pressure, which is determined by Paschen breakdown. Measurements indicate that contamination with 30% argon or 20% air will reduce maximum operating pressure by 50%. At the same time, minimum operating pressure, which is determined, in part, by the ionization cross section of the gas mixture, is reduced. The discharge itself acts as a pump for chemically active contaminants such as air and water. This is a result of sputtering produced by energetic ions striking the cathode surfaces. Measurements with the 4 cm x 40 cm gun indicate that the discharge pumps air at a rate of about 5 x 10^{-3} Torr-liter/sec. This corresponds to a reduction in the partial pressure of air by 20 mTorr in 1 min. Thus, once the outgassing or leakage rate has been reduced below this level by conditioning (cycling between gun operation and evacuation) the discharge will remove any further contamination. Consequently, the gun continues to clean up so that stable, consistent operation becomes more likely. After conditioning with a foil window, however, the possibility of leaks and outgassing increases, so that the conditioning process takes longer.

D. <u>Uniformity of the Extracted E-Beam</u> — The 4 cm x 40 cm plasma cathode e-gun was studied in three different experimental configurations to determine and improve the uniformity of the output electron beam. In the first set of experiments, the cathode and grid structure of the gun was placed in a bell jar and the uniformity of the plasma cathode discharge measured with a single, movable Faraday cup ion probe. Next, the e-beam current density distribution was studied with 21 Faraday probe current collectors placed at different positions in the 4 cm x 40 cm e-beam pattern and mounted on a solid collector plate bolted to the e-gun. Finally, a 100 keV e-beam was extracted through a thin foil window and probed by means of a single Faraday cup current collector, which could be moved continuously along the 40 cm gun dimension in the center of the pattern. In all three experimental arrangements,

51

small endplates were placed within and near the ends of the hollow cathode chamber to alter and improve the observed beam uniformity. These end-plates could be biased at a fixed voltage, allowed to float, or connected electrically to the hollow cathode.

The beam density and beam uniformity measurements were inconclusive due to the impossibility of determining the differences in the responses of the 21 Faraday probes. The bell jar and foil extrac-tion measurements, in which a single, movable current collector is used, were useful and the details of these two experiments are presented below.

1. Low-Voltage Bell-Jar Experiments

To study the effects of structure modifications to the e-gun on the expected current-density profile, the cathode-grid struc-ture of the 4 cm x 40 cm e-gun was placed in a vacuum bell jar. In this configuration, the plasma density of the hollow-cathode discharge was studied by measuring the spatial variations of an extracted ion beam. The justification for this experimental approach is based on two assumptions:

- The spatial variation of the extracted e-beam depends primarily on the electron density in the hollow-cathode discharge which in turn equals the ion density for a neutral plasma.

- The control grid (G2) and the plasma, with a Debye length of ≈ 0.5 mm, isolates the condi-tions in the hollow cathode region from the acceleration region so that operating at high voltages with an extracted beam does not strongly affect the conditions within the hollow cathode.

The ion density in the hollow-cathode discharge was monitored by a modified Faraday cup probe mounted on a rod located ≈ 0.7 cm from the control grid which could be moved continuously along the 40 cm dimension of the structure. The Faraday cup had a collecting aperture of 0.32 cm^2 (6.35 mm diameter); a suppressor grid in front of the collector was operated with a negative bias of about 20 V (with respect to the collector) to minimize the effects of secondary emission from

52

the collector plate. The collector was run at a negative potential of 20 V relative to the cup and aperture. The sliding contact for an 8.5 potentiometer was connected to the rod which moved the probe; this allowed the position of the probe to be continuously monitored. A continuous analog recording of ion current versus position (as determined by the voltage across the potentiometer) was made using an x-y recorder. Over fifty such recordings were made under many different gun conditions and configurations.

The gun structure was modified by placing two 0.012 in. thick stainless-steel plates in the hollow cathode can. They were oriented normal to the axis of the gun, and at the ends of the 40 cm aperture of the gun. These 4.5 in. diameter endplates were circular, except for a segment cut off to clear the screen grids (G1 and G2). This size provided a 3/16 in. clearance between the interior of the hollow cathode and grid surfaces; the endplates were therefore electrically isolated from the rest of the cathode parts.

Tests were run with and without endplates. In separate tests, the endplates were allowed to float, were connected to the cathode, or were maintained at a fixed voltage (50 to 400 V) with respect to the cathode. These experiments showed that the plasma density in the hollow-cathode discharge could be modified in a predictable manner due to the presence of the endplates. Without the endplates, the plasma density fell off from the uniform midgun value to near zero at the ends of the gun aperture, with a transition region of 4 to 8 cm. Operation with the endplates biased to 250 to 300 V or floating (where the potential floats up to the plasma potential, which is near the anode grid voltage of 400 V) gave an increase in the plasma density near the ends of the 40 cm aperture, so that the fall-off region was approximately halved. In the best cases, the uniformity of the observed ion density was ±5% over the central 80 to 85% of the longitudinal aperture. Variations of ±10% to ±20% were more typical.

The observed increase in plasma density near the ends of the beam aperture is believed to be due to changes which plasma species experience in the potential near the walls. In the normal case, when the edges of the aperture are at cathode potential (which is also the case when the end plates are operated at cathode potential), a sheath on the order of a centimeter thickness develops which reflects electrons back into the interior of the hollow cathode and causes the plasma density in the sheath region to be low. When the positively biased or floating end plates are present. electrons no longer experience the reflection of the sheath near the end plates and the plasma density increases.

It was observed that contamination effects played a major role in determining the uniformity of the plasma density. The bell jar is not the clean environment in which an electron gun is meant to run. The gun was usually so badly contaminated after a couple of data runs that the observed plasma density became grossly nonuniform (even for fresh gas fills) and the gun would have to be disassembled and cleaned. This occurred even when the diffusion pump line was LN trapped. A microprobe analysis of the contaminated parts was not conclusive in showing that the contamination was due to pump oil or vacuum grease from the bell-jar seals. Nevertheless, due to these contamination problems, it was decided to continue tests of the endplate configurations with the gun in a clean, high-vacuum environment at high voltage and observing an extracted e-beam.

2.   Extracted Beam Measurements at High Voltage

The 4 cm x 40 cm plasma cathode e-gun was operated in the configuration for which it would be used to pump e-beam sustained lasers. In this configuration, the e-beam was extracted through a 4 cm x 40 cm thin foil window. The window was made of Kapton, coated on both sides with a thin layer of aluminum, and had a total thickness of 0.0005 in. The chamber downstream from the foil was evacuated: it housed the moving Faraday cup probe used in the bell-jar experiments. This probe was grounded through a low input

54

impedance current to voltage converter and thus acted as an electron collector. As before, the position of the probe was monitred by putting a known voltage across a potentiometer, the moving contact of which was connected to the moving rod and probe, and reading the voltage on the contact. Probe diameter was 6.35 mm. In addition to the movable probe, a solid 6 cm x 45 cm aluminum collector plate which collects (approximately) the total transmitted e-beam was located behind the moving Faraday cup probe. The diagnostics box, the moving probe, and the collector plate are shown in Figure 23.

Figure 23. The diagnostics chamber.

No attempt was made to cool the foil and, consequently, it was necessary to operate at a low current density for a short duration at 100 to 120 kV. Satisfactory operation at ≈ 100 $\mu A/cm^2$ for ≤ 1 sec was obtained, although the current density distribution data were taken at ≈ 30 $\mu A/cm^2$. At each probe position, the probe current signal received was displayed on a storage oscilloscope, along with a signal proportional to the total beam current drawn, so that a reference for each probe position reading could be maintained. Data was taken with endplates both floating and connected to the cathode.

Figure 24 presents the results for the floating endplate case. The data from two runs, taken on different days and with different helium gas fills, are included. Good data reproducibility is seen, and the beam is uniform within ±5% over about 15 cm to 20 cm and ±10% over 25 cm. This can be compared to the similar data taken for the case in which the endplates were tied to the cathode (as shown in Figure 25). The two sets of results are compared in Figure 26 (which plots the averaged results for each operating condition). A small change between the two data sets is apparent. This change, a slight increase in the density nearer the edges of the beam, is consistent with the results of the bell-jar experiments.

These results show that the extracted beam of the plasma cathode electron gun is very uniform, ±5%, over the central region of the gun aperture. Near the edges, 5 cm to 10 cm away, the current density decreases, probably due to sheath effects and potential gradients present at the gun in those regions. For a larger gun of 100 cm to 200 cm length, these end effects represent a nonuniformity over a small fraction of the aperture and are tolerable. Endplates could be installed to help decrease these edge effects if operated either with a fixed potential (250 to 300 V) or allowed to float toward plasma potential. The latter case is preferred since no additional lead in the high-voltage feedthrough would be required.

3.   Pulsed Operation of the 4 cm x 40 cm E-Gun

Although the two guns with rectangular geometry electrodes, the 3 cm x 10 cm and 10 cm x 15 cm guns, were only operated in

56
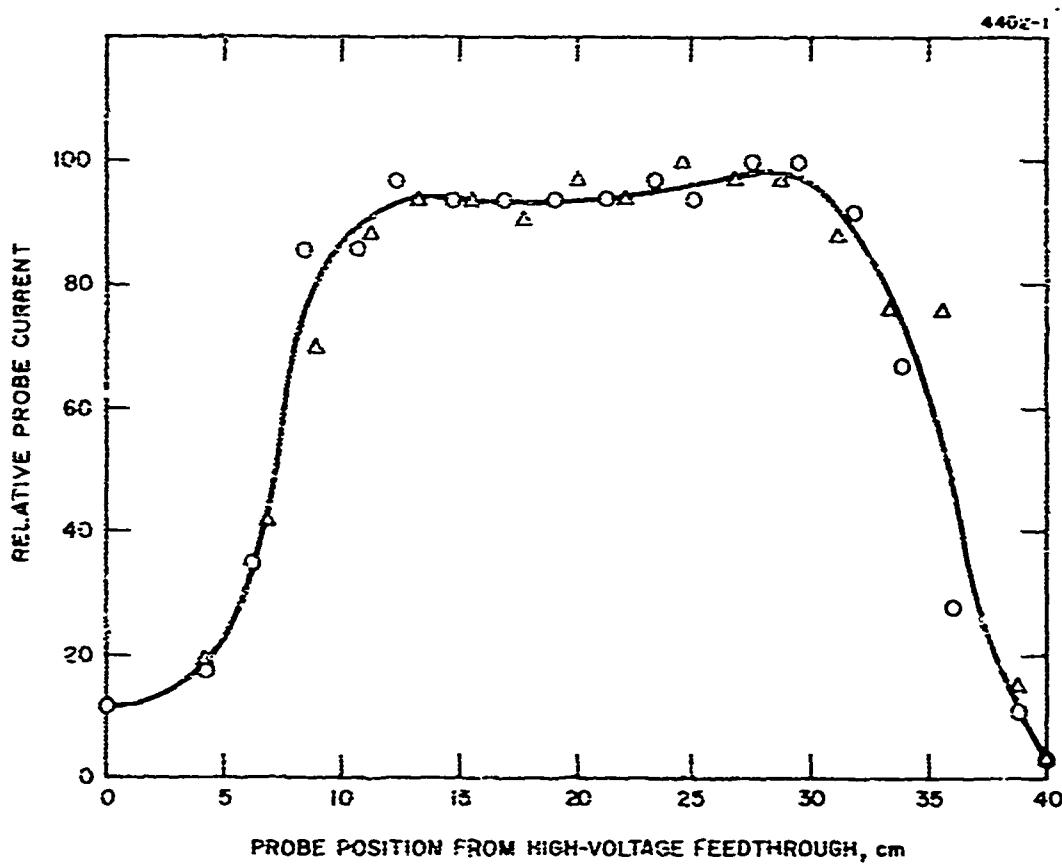
Figure 24. Relative transmitted beam current versus probe position with endplates tied to the cathode and with a beam voltage of 100 kV and an average current density of 30 μA/cm^2.

57

RELATIVE PROBE CURRENT

PROBE POSITION FROM HIGH-VOLTAGE FEEDTHROUGH, cm
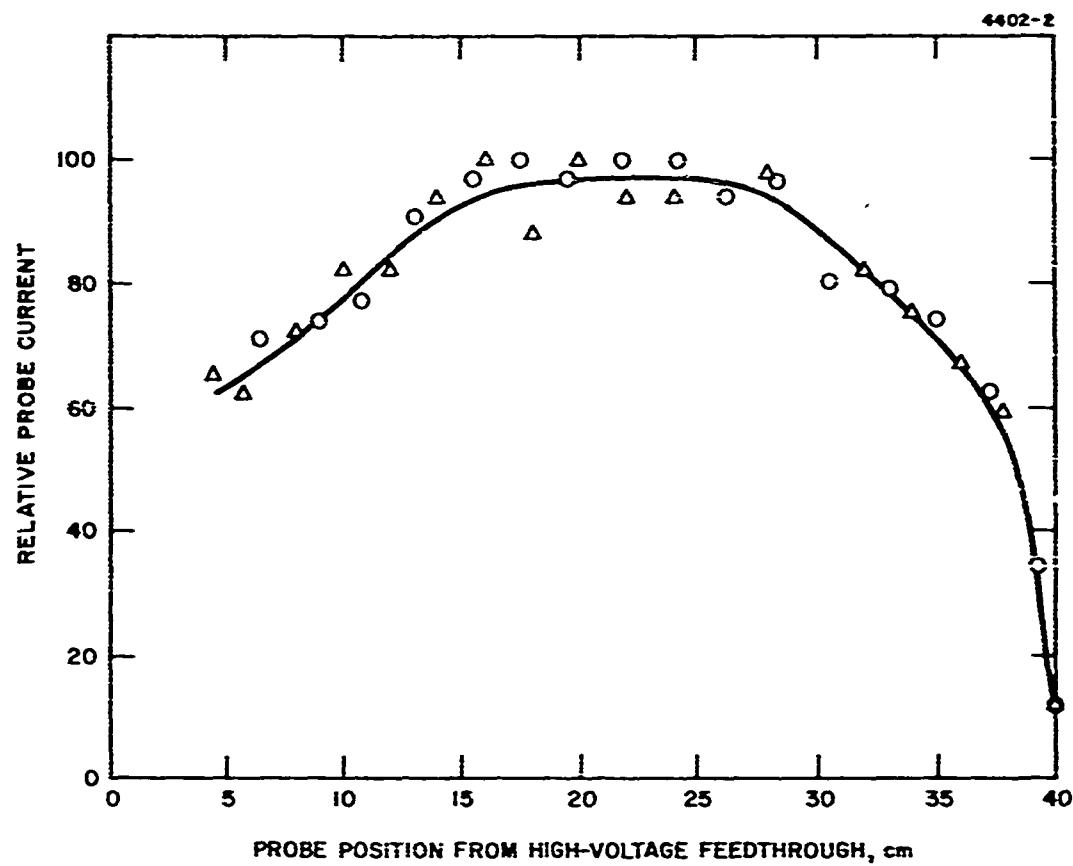
Figure 25. Relative transmitted beam current versus probe position
with endplates floating and with a beam voltage of 100 kV
and an average current density of 30 $\mu A/cm^2$.

58

a pulsed mode, careful attempts were not made with them to determine the maximum possible extracted current density and the output beam uniformity. For this reason, the 4 cm x 40 cm coaxial gun was run in an experimental arrangement in which both the spatial and the temporal characteristics of the pulsed (10 µsec to 50 µsec pulse widths) extracted e-beam could be studied. For these pulsed experiments, the mechanical arrangement was the same as that for the extracted cw beam experiments described above. In particular, the aluminum-coated Kapton foil (0.0005 in. thickness) was mounted on an 80% transmitting aluminum support structure. The total beam transmission for the foil structure and the high-voltage anode grid is estimated to be 33% at 100 kV and 40% at 150 kV. The same beam diagnostic arrangement as shown in Figure 23 was used.
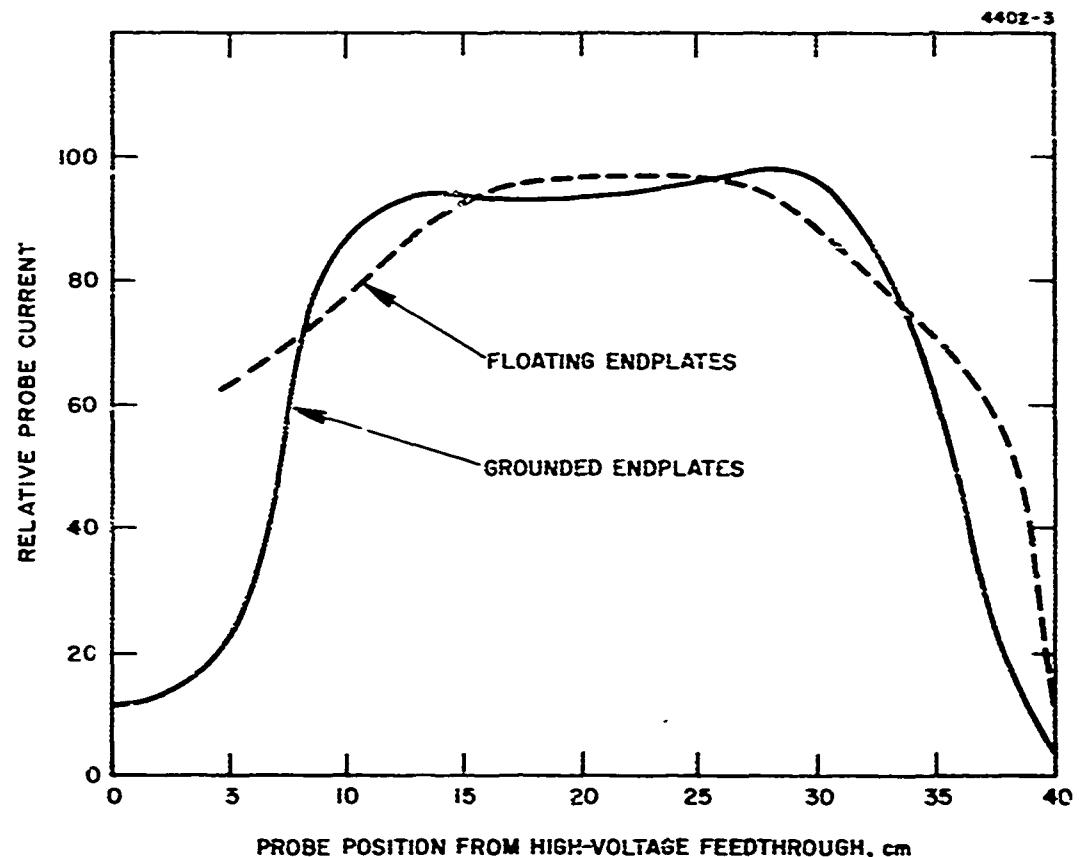
Figure 26. Comparison of spatial distribution of output current.

59

The electrical schematic is shown in Figure 27. The 115 Vac used with the igniter power supply and the Velonex Model 350 pulse generator is supplied at high voltage through an isolation transformer. The igniter, which is on continuously, supplies a current greater than 5.4 mA (the experimentally determined minimum value to ensure proper operation). Pulsed operation of the anode grid and the hollow-cathode discharge is effected by the Velonex pulse generator. The Velonex output, prf, and pulsewidth are controlled at low voltages by the operator and transmitted by an optical transmission line to the high-voltage environment of the Velonex. Pearson current transformers are used to measure the current flowing out of the high-voltage energy storage unit (I_{ps}) and the current collected by the solid collector plate (I_c). The current, I_{ps}, is the net current leaving the control grid and incident upon the foil assembly. At lower beam voltages (<10 kV), additional current loops and voltage probes were used to monitor anode current and voltage and cathode current. The control grid voltage could be continuously varied from 0 to 45 V (negative with respect to the anode grid as shown).

In this configuration, the attainment of the highest current density (I_{ps}, the current into the foil, or I_c, the current collected at the collector plate) was studied. Studies of the beam spatial uniformity were not attempted. The most notable results obtained were:

- Maximum current output at high voltages (100 kV) and 20 to 30 µsec pulses:

$$I_{ps} \approx 10 \text{ A (current into the foil)}$$

$$I_c \approx 1 \text{ A (current collected by the collector plate representative of, but not equal, to the total extracted current)}$$

- Maximum current output at lower voltages (<60 kV):

$$I_{ps} \sim 30 \text{ A} .$$

60
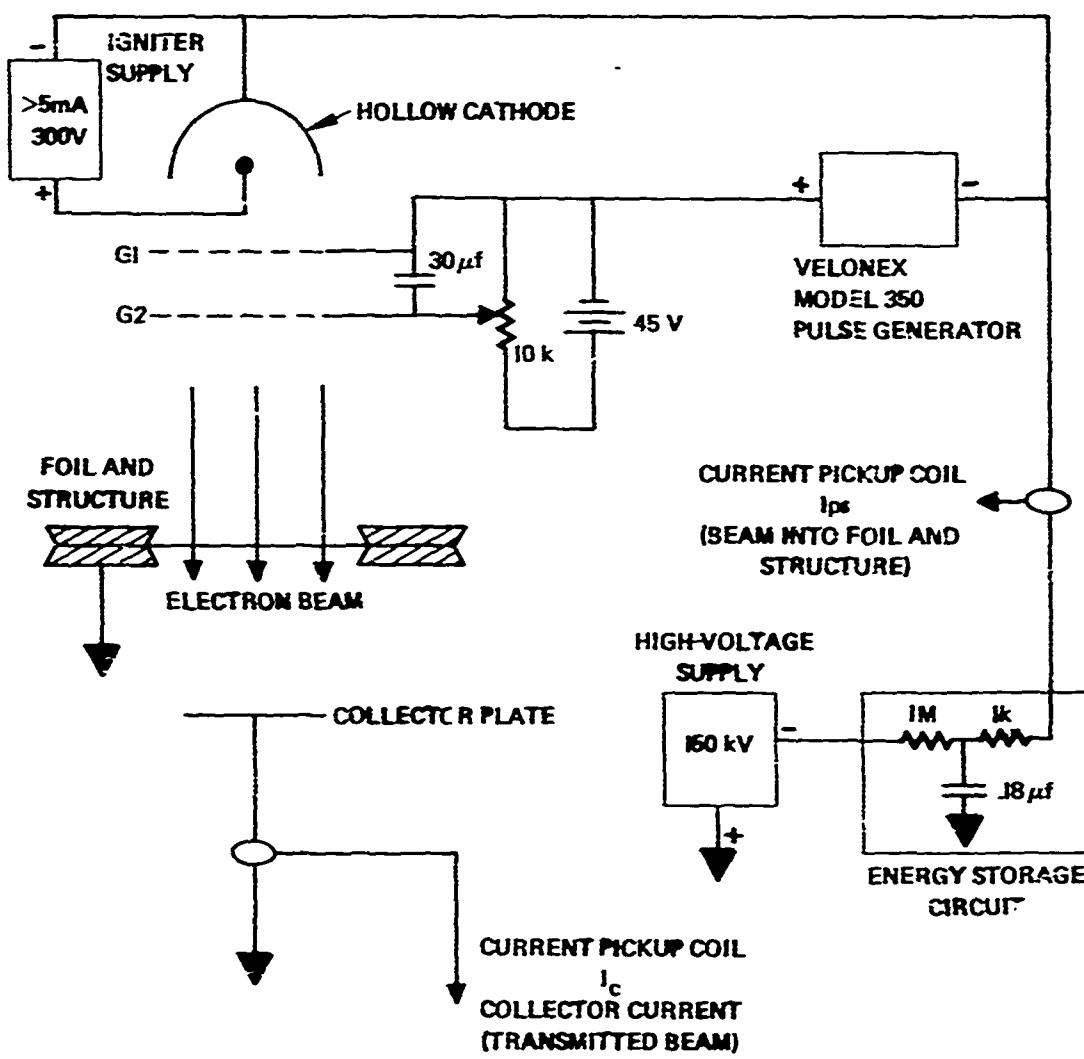
Figure 27. Schematic of experimental arrangement.

Stable operation of the gun at high voltage was made difficult by the onset of arcing and beam current oscillation phenomena. The exact nature of these effects varied in a generally nonreproducible manner. Although the exact cause of these arcs and oscillations is not known, similar phenomena were observed earlier with the 2 cm x 10 cm and 10 cm x 15 cm guns at the same range of current densities. In addition, there was some evidence that gun cleanliness played an important part in the arc and oscillation thresholds. Unfortunately, at low pressures, where more stable high-voltage operation could be expected, the discharge would not light reproducibly.

Figure 28 shows a typical oscillogram for operation of the gun at 100 kV where the pulse amplitude of the Velonex and the control grid voltage are adjusted to keep the gun current levels below arc threshold. The upper trace is the collector current for the beam transmitted through the foil (scale 100 mA/div) and the lower trace is I_{ps} (scale 1 A/div). As stated above, the highest peak current extracted from the gun was limited by arc and/or oscillation phenomena. Reliable operation of the gun with a pulse length of 20 to 50 μsec was demonstrated, and, depending on gun cleanliness, the current density upstream of the foil (I_{ps}) could vary from 10 to 70 mA/cm^2. These values of current density are similar to those obtained in operating the rectangular geometry 2 cm x 10 cm and 10 cm x 15 cm guns. In these guns the maximum current density obtainable was also limited by similar oscillation/arcing phenomena, even though these guns were of considerably different mechanical design. Circuit effects may be ruled out as a determining factor for the oscillatory behavior of the gun. Recent data have shown how, with the same external circuitry, the gun may oscillate at low or high frequency. In addition, changing the circuit had no discernible effect.

4899-4
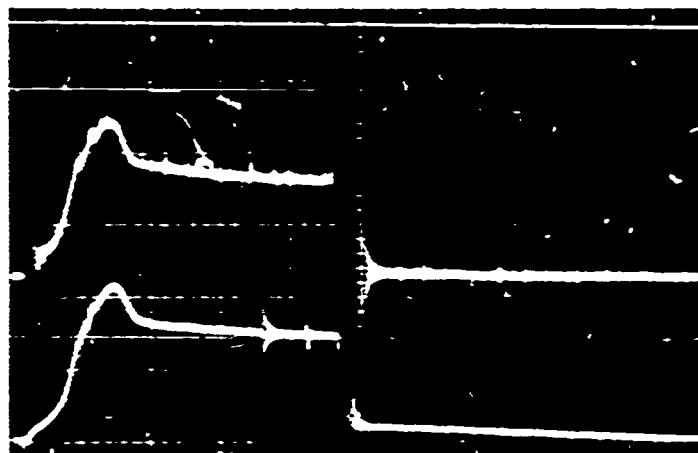
Figure 28.
Pulsed current output of the 4 cm x 40 cm
coaxial geometry plasma cathode electron
gun at 100 kV. Top Trace: Current trans-
mitted through a 0.0013 cm thick aluminum
coated Kapton foil. 100 mA/div. Bottom
Trace: Current into the foil and support
structure. 1 A/div. Sweep speed: 10 μsec/div.

Since, from several different pulsed plasma cathode e-guns, we
have obtained similar maximum current densities, it may be that the
current density output of 50 to 70 mA/cm^2 represents a limit to the
capability of the gun. So far we do not know any of the basic mechan-
isms which limit gun output current, or what are the causes for and
the nature of the observed oscillations. It is to be noted than an
approximate calculation of the plasma current density in the hollow-
cathode discharge. $j_p = (1/4) \eta_e e V_d$, where

j_p = the current density in A/cm^2

η_e = plasma density in the discharge in cm^{-3}

e = electronic charge in coulombs

V_d = average electron velocity in cm/sec.

yields $j_p \approx 30$ mA cm^2 for values of η_e and V_d typical for the plasma
cathode discharge ($\eta_e = 10^9/cm^2$, $T_e \sim 4$ to 10 eV). This value of j_p is
in the same range as the observed threshold for arcing and oscillation.

Whatever causes the oscillation/arcing phenomena, the maximum pulsed current density obtainable from the plasma cathode e-gun is limited by the effects to ≈ 50 mA/cm^2. In addition, in repetitively pulsed operation, the maximum average current density must be limited to ≈ 1 mA/cm^2 for stable, high-voltage results.

Plans for further tests to characterize the pulsed operation of the plasma cathode electron gun were abandoned in favor of the development of the ion plasma electron gun (as described in Section III). As will be discussed, the pulsed operation of the ion plasma e-gun has far more favorable characteristics than the plasma cathode gun.

D.   Conclusions

The plasma cathode electron gun was developed on this program to become a gun which, for cw operation, is a strong competitor to the thermionic e-gun. Because of this development, large-scale plasma cathode electron guns have been built and operated to pump e-beam sustained CO_2 laser systems. Other plasma cathode guns have been used with molecular chemical lasers and to investigate new molecular laser systems. Based on the guns tested in this program, the plasma cathode gun has the following characteristics.

- **Beam voltage**   Up to 160 kV.

- **Beam Current density**   Up to 400 μA/cm^2 (cw) into the foil window. Power supply and foil cooling limitations prevented tests at higher currents.

- **Beam uniformity** $\pm 5\%$ over the beam aperture except for a fall-off at the ends of the aperture, where the beam density drops over 5 to 8 cm.

- **Gas pressure**   30 to 50 mTorr of helium.

While operating the plasma cathode guns under high-voltage conditions and extracting a beam through the foil, outgassing from the foil and other parts of the gun subjected to the high-energy electron flux has occasionally caused Paschen breakdown with a resulting arc to an rupture of the foil window. In the existing guns, a gas pressure

of 30 to 40 mTorr of helium is required to produce enough ionization to supply the e-beam, especially if a large extracted current is desired. The Paschen breakdown limit of the gun is approximately 50 to 60 mTorr in pure helium, but the presence of contaminant gases with a lower Paschen characteristic could lower the arc threshold pressure considerably. For this reason, operation of the plasma cathode gun or other type of gun at a lower pressure (<10 mTorr) would be desirable. At these low pressures, the ratio of cathode surface area to extracted beam area must be increased so that the hollow cathode discharge can be lit at reasonable voltages.

As a result of the progress on this program, two plasma cathode guns have been built on other programs to pump e-beam sustained lasers. Both of the guns in these cases were designed so that the hollow-cathode beam-extraction area ratio was ≈ 6 times larger than that in the coaxial guns studied in this program. Both new guns are cw guns and have operated reliably at helium gas pressures ≤ 10 mTorr, with a beam current density in excess of 400 $\mu A/cm^2$ (up to 800 $\mu A/cm^2$ for short time periods) at 150 kV. One gun, with a 5 cm x 200 cm extracted beam, built at HAC Culver City for the ARPA/Lincoln Labs Laser Radar Power Amplifier, has operated at 150 kV for runs as long as 15 min. Based on all these results, the advantages of the plasma cathode e-gun over a thermionic gun include:

- Simple, rugged construction — No inherently delicate heater elements required: thermal stress problem minimized: smaller size.

- Instantaneous startup — No warmup time: beam extraction obtained immediately after discharge ignition (which occurs in ≈ 1 μsec).

- Relative insensitivity to contamination — Foil rupture or leaks do not poison cathode surfaces, although purity of the fill gas and vacuum integrity need to be maintained for high-voltage operation.

- High efficiency — Consumes less power from supplies floating at high voltages.

- Low cost — Fewer parts. simpler, easier to scale.

65

A possible disadvantage of this gun is that it is gas-filled and and not a vacuum gun. This means that, at high voltage, care must be taken to maintain a clean helium environment free of large amounts of contaminant gases. As described above, using larger aspect ratio guns (more hollow cathode volume for the same current output) decreases the pressure and eases the high-voltage constraints. The ion plasma electron gun (described in Section III) also operates at low helium pressure, which makes it better suited for high-voltage operation and an attractive alternate to the plasma cathode gun. For cw applications, the plasma cathode gun has proven itself. For pulsed operation, the ion plasma gun has been demonstrated to be clearly superior to both the plasma cathode and the thermionic guns, and competitive with cold-cathode, field-emission types of guns. As mentioned above, during the pulsed plasma cathode tests, the decision was made to concentrate all efforts toward developing the ion plasma gun, even before all pulsed tests of the plasma cathode could be completed.

III.   THE ION PLASMA ELECTRON GUN

The ion plasma electron gun is a new type of electron gun which is capable of operating at lower gas pressures than most other gas-filled guns. This lower pressure means that the ion plasma e-gun is capable of the high-voltage operation and high current fluxes applicable to e-beam sustained laser systems in pulsed and cw operation. On this program, the initial experimental re. lts were obtained. After the end of the contract, the theoretical model of the gun was derived and additional data points taken to corroborate the model; this work was carried out on company IR&D funds.

A.   Theory of Operation

A schematic of the ion plasma electron gun is shown in Figure 29. In this gun, a low-voltage plasma is struck near the anode, and this plasma acts as a source of ions. The plasma may be obtained by any one of several means, including a thermionic diode discharge,[7] a hollow-cathode discharge,[8] or a thin-wire discharge. Thin-wire discharge, the method shown in Figure 29, will be described more fully below. A fraction of the ions produced in the discharge are accelerated to the cathode (negative high voltage of as much as 400 kV), where they collide with the electrode surface and produce secondary electrons. These electrons are then accelerated back toward the anode, experiencing few collisions in the process of passing through the low-pressure gas (mean free path for 100 kV electrons in 20 mTorr of helium is ≈ 100 m^2). This electron beam then passes through the thin foil window and into the laser chamber or region where the beam is to be used.

Only the thin-wire discharge, of the three previously mentioned ways of producing the discharge plasma, operates at a pressure low enough to be compatible with high-voltage gun operation and can be used with a compact design configuration. The thin-wire discharge, which has been experimentally studied by McClure,[9] can operate at low pressure because the thin wire permits highly efficient electrostatic trapping

67

of electrons to sustain the discharge. In this discharge, electrons are trapped in the electric field near the thin wire (at a positive voltage of 400 V) and form helical orbits around the wire. These orbits allow the electrons to attain long path lengths so that ionization of helium atoms can occur (ionization mean free path in 10 mTorr of helium for 400 eV electrons is 70 cm).[2] This mechanism results in a limited sustaining generation of electrons. In the present experiments, this thin-wire discharge has been operated with pressures as low as 2 mTorr in helium.

An array of thin wires (each wire separately driven) in the ion plasma electron gun can be distributed across the beam aperture and in the discharge region. Since the depth of the discharge region may be as small as a centimeter, it will not add much to the size of the gun. A hollow-cathode discharge is also an efficient ion source, but for operation at pressures <10 mTorr, the ratio of hollow-cathode surface area to extraction area must be increased significantly to obtain meaningful currents. A larger area ratio will increase gun size. Using a thermionic cathode discharge as an ion source allows low-pressure operation, but again size must be significantly increased to accommodate the cathode heaters.
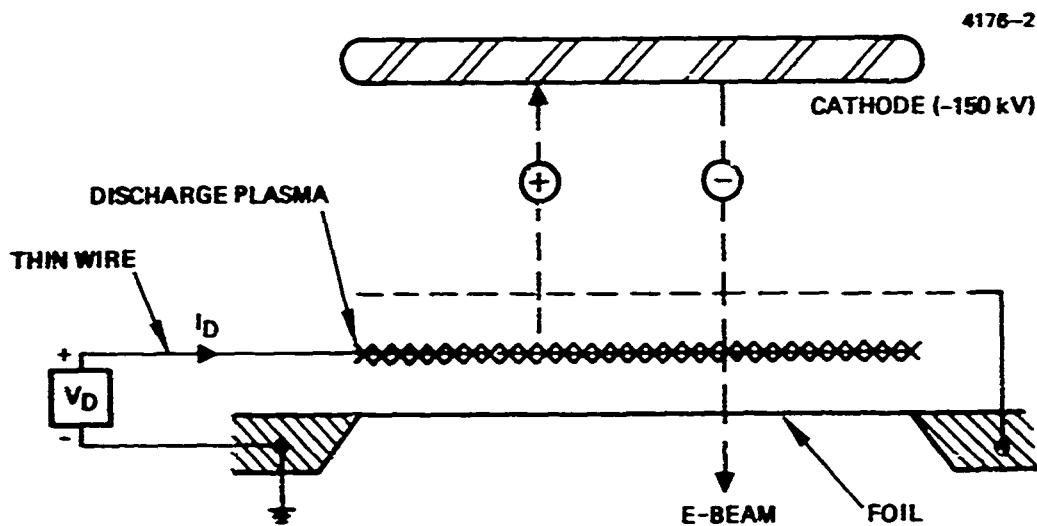

Figure 29. Ion plasma e-gun schematic.

68

A simple theoretical model of the gun's operation is presented below. The thin-wire discharge current, I_D, produces equal amounts of plasma electron and ion current (0.5 I_D each) in the discharge region. Most of the ion current is collected at the ground potential surfaces (i.e., the foil, ion extraction grid, and walls of the region); the rest passes through the ion extraction grid and into the high field region, where the ions are accelerated to the cathode. A fraction of the ion current is directed toward the grid. This fraction is estimated to be ≈ 0.25 using a simple geometrical model and neglecting the fringing through the grid of the large field in the acceleration region. The effective potential at the grid, as seen by the ions, relative to the thin wires is $V_{grid} = -V_{anode\ wire} - V_{cathode}/\mu$, where $\mu \approx 10^3$ is the amplification factor of the grid[6] so that $V_{grid} \approx -400\ V - 125\ V = -525\ V$ (for 125 kV operation). This means that the high cathode voltage increases the effective potential of the grid by $\approx 25\%$, which indicates that fringing of the large field into the plasma discharge region does occur and will increase the amount of ion current directed toward the grid. This increase is offset by the fraction of the ion current intercepted by the grid (20% in the device tested) so that the ion current passing the grid is approximately $I_+ \approx 0.125\ I_D$. At the cathode, η_s secondary electrons are produced for each incident ion. This secondary emission coefficient, η_s, has been measured[10,11] to be from 10 to 14 but in these measurements the ions were directed onto the steel surface in a field-free drift region. In the present case, a field of 30 kV/cm exists at the cathode, which means that η_s may be larger than the reported values. In any case, the electron current incident on the foil window will be $I_e \approx (1/8)\ \eta_s\eta_g I_D$, where η_g = ion extraction grid transmission (≈ 0.3 present device). From these preliminary considerations, the prediction would be that $I_e \approx I_D$. At beam voltages above 120 kV, a foild window and support structure may be built so that ≥ 0.8 to 0.9 of I_e is transmitted into the laser region.

In fact, as will be described in the next section, since the relationship between I_e and I_D is not linear, so the more complicated physical mechanisms must be included in an accurate theory of operation for the

ion plasma electron gun. Some of the mechanisms which may be important to the operation of the gun, and which could help explain the observed data, will be presented in Section III-D.

The efficiency of the gun is dependent on the ratio of (1) the energy delivered by the high-voltage supply to the electrons to (2) the total energy delivered to the ions and electrons. Since the energy needed to drive the plasma discharge is negligible compared to that delivered by the high-voltage supply, the plasma-supplied energy may be neglected in calculating gun efficiency (the plasma discharge voltage is ≈ 400 V and, since $I_D \approx I_e$, the plasma discharge energy is $\approx <1\%$ of the energy supplied by the high-voltage supply). From these considerations, total gun efficiency is

$$\eta_T = \frac{\eta_s}{1 + \eta_s} \quad \eta_g \eta_f \quad ,$$

where

η_s = secondary emission coefficient

η_g = ion extraction grid transmission

η_f = foil window structure transmission .

At high beam voltages (>125 kV), η_T will be around 60%.

The ion plasma electron gun has important potential advantages for application to e-beam pumped laser systems. These advantages include:

- High-voltage operation Because the ion plasma e-gun can operate with a helium gas pressure below 10 mTorr, operation with a beam voltage in excess of 400 kV may be anticipated.

- High current density A current density of between 5 and 10 A/cm^2 may be estimated for beam voltages of 300 kV or higher. The maximum current density obtainable may be limited by space charge effects on the ion beam being extracted from the discharge region.

70

- **CW and pulsed operation** The ion plasma
  e-gun has operated both cw and in the pulsed
  mode with pulse lengths as short as 0.5 µsec.
  Unlike the cold-cathode field-effect guns, the
  output current density does not fall with
  increasing pulse length, due to limitations of
  the gun mechanism. Instead, the average cur-
  rents obtainable are set by foil window cooling
  and power supply limitations.

- **Monoenergetic beams** Even at high ion energies
  secondary electrons emitted are expected to
  have initial energies less than 40 eV.[11,12] At
  the high beam energies anticipated, this
  represents a small fractional energy spread.
  Because of this and the fact that a dc high
  voltage supply is used, a very monoenergetic
  e-beam may be expected which will result in
  good foil penetration. Low-energy electrons
  (which result from the rise and fall of the supply
  voltage and are present with field-effect cold-
  cathode guns) will not be present with the ion
  plasma e-gun.

- **Gun control with electronics at ground potential**
  The ion plasma gun is controlled by the plasma
  discharge, which operates at about 400 V above
  the ground electrode (anode) of the gun. This
  means there is no need for the electronics to
  run the gun to be floated at high voltage, as is
  necessary with thermionic and plasma cathode
  e-guns.

- **DC high-voltage supply for repetitively pulsed
  operation** For applications requiring repeti-
  tively pulsed operation, the ion plasma gun
  will operate with a dc high-voltage supply.
  Field emission cold-cathode e-guns require a
  repetitively pulsed Marx-bank high-voltage
  supply.

- **Scalability** Based on experience on this pro-
  gram with the wire discharge, there appears
  to be no reason why the ion plasma gun cannot
  be scaled to produce large-area beams.

B.   Experimental Arrangement

The ion plasma gun was tested experimentally during the last seven months of this contract. The experiments were devised to test the gun in as flexible a configuration as possible. For this purpose, the 4 cm x 40 cm plasma cathode e-gun (Figure 8) was modified to operate as an ion plasma e-gun. The modifications required were relatively simple and were accomplished more quickly than the design and fabrication of a new gun device could have been. The ion plasma gun which resulted from these modifications is not an optimum design, but it has proven itself to be a useful test vehicle and has been operated up to 130 kV.

A schematic of the test device is shown in Figure 30. In comparison with Figure 8, the modifications to the original plasma cathode gun have included:

- Replacing the anode and control grids of the plasma cathode gun with a single stainless-steel plate which closes off the hollow cathode and is the secondary electron emitting cathode surface.

- Adding a thin-wire discharge plasma generation region.

In the gun, the high-voltage acceleration region is defined by the flat portion of the cathode surface and by the ion extraction grid (located at the boundary between the plasma generation and acceleration regions). This grid is made of fine stainless-steel wire mesh: it has approximately 80% transmission with a wire size of 0.001 in. and a square mesh size of 0.025 in. The acceleration gap is 4 cm. The foil support structure used is the same as that described previously: 0.001 in. thick aluminum foil windows were used in these experiments. The gun was mounted to the plexiglas diagnostics box described previously (Figure 23) so that current density uniformity measurements could be taken with the moving Faraday cup current collector.
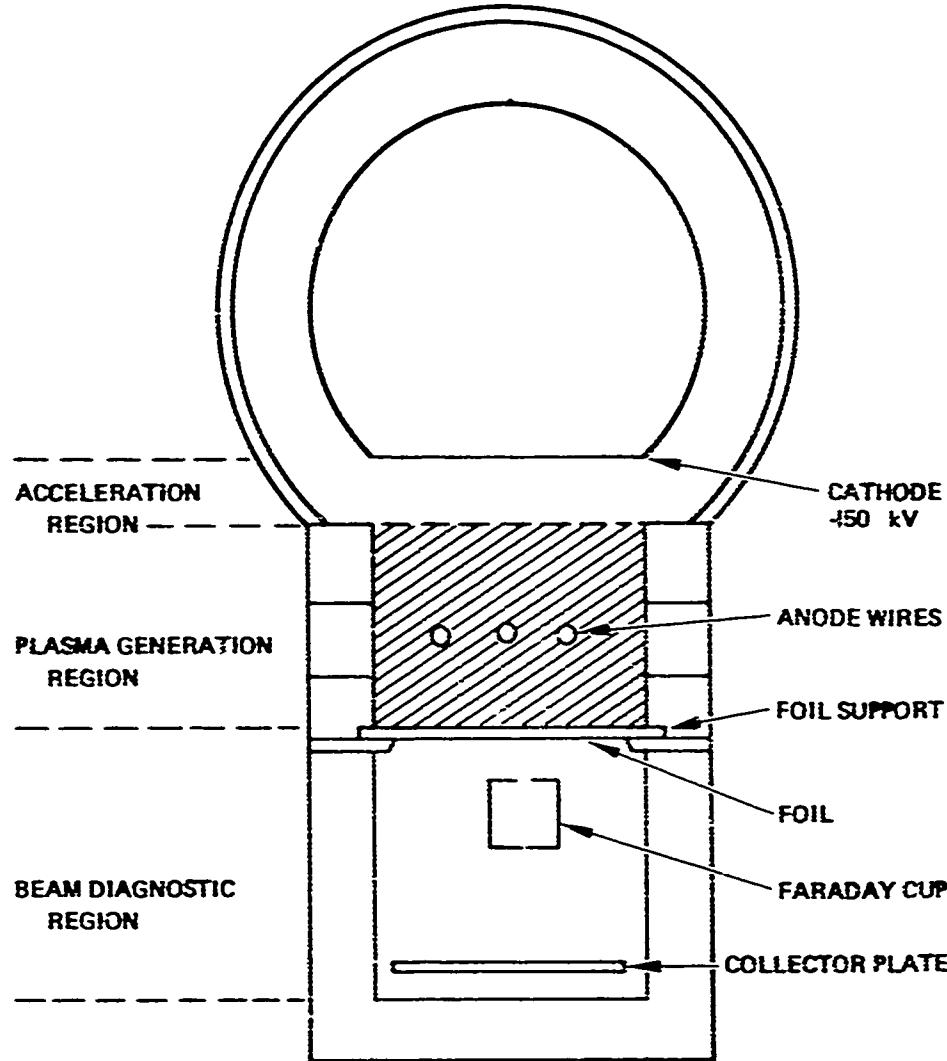
Figure 30. Ion plasma e-gun test device.

73

ANODE WIRES

a

WIRES
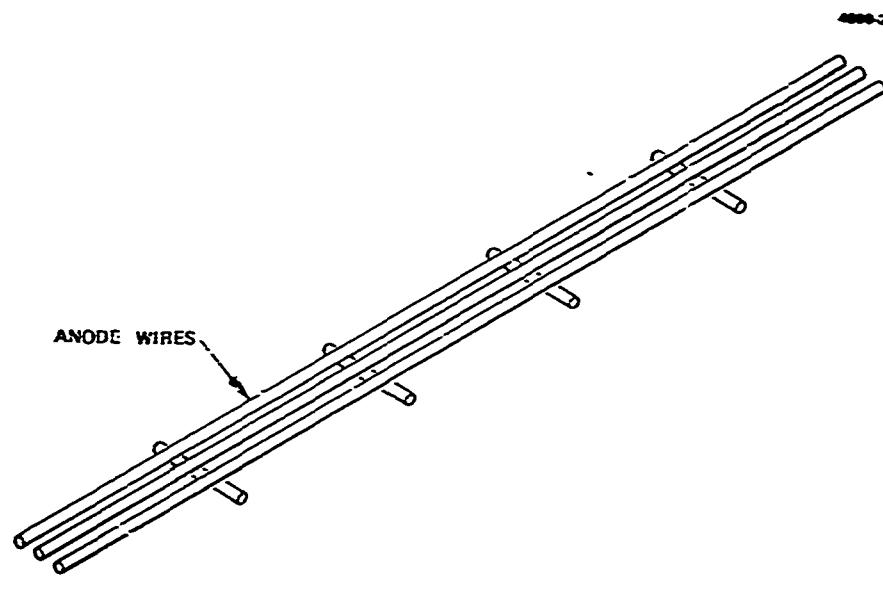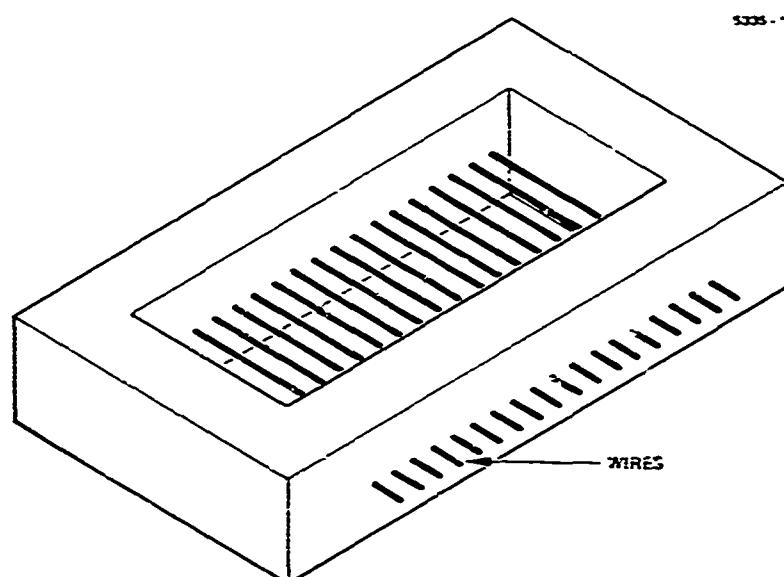
b

Figure 31. Schematic of the two different thin anode wire alignments used.

The plasma generation region is a thin-wire discharge chamber with a transverse cross section of 4 cm x 4 cm. Two different thin-wire configurations were tested. In the first, three individual 0.3 mm diameter tungsten wires were placed 1 cm apart running longitudinally along the discharge chamber. Four wires were also run transversely across the discharge region and located 1.6 mm below the plane of the longitudinal wires. This configuration is sketched in Figure 31(a). Data were taken with only the longitudinal wires being driven: the transverse wires were, on occasion, used as Langmuir probes. For the second configuration, as shown schematically in Figure 31(b) and photographically in Figure 32, seventeen transverse wires were used, with the center wire being available for use as a Langmuir probe. This second configuration was used to increase the amount of anode current and to decrease the system inductance for short pulse, high current tests.

The ion plasma electron gun was operated in two different modes: a quasi-cw operating mode in which the thin wire anode discharges were switched on for 5 to 150 msec and a short-pulse mode yielding anode wire current pulses of 2 to 5 μsec FWHM. In the first case, for which the test schematic is given in Figure 33, the anode wire discharges were switched on and off by reed relays. In this case, the maximum pulse length was determined by the energy storage capacity of the high-voltage power supply and by foil heating constraints. Care was also taken in this operating mode to ensure that the three anode wires (in quasi-cw operation, only the 3 anode wire configuration was used) carried equal currents.

In short-pulse operation, the test circuitry was the same, except for the way the thin-wire anode discharges were driven. In this case, each wire was driven by its own 0.01 μf capacitor, charged to 2 kV, and switched by a thyratron. A single thyratron switched all the wires. In the 17 wire configuration, the ratio of total current switched to the current in one single wire indicated that all wires carried approximately the same current. The total current capacity of the thyratron used was about 300 A.

75
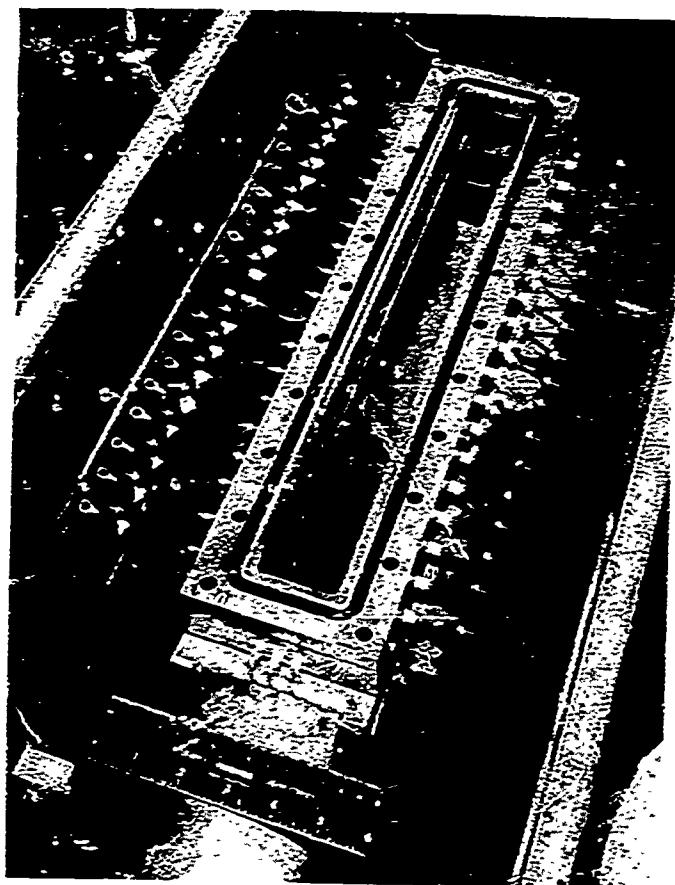
Figure 32.
Photograph of the thin-
wire discharge chamber
with seventeen trans-
verse anode wires.
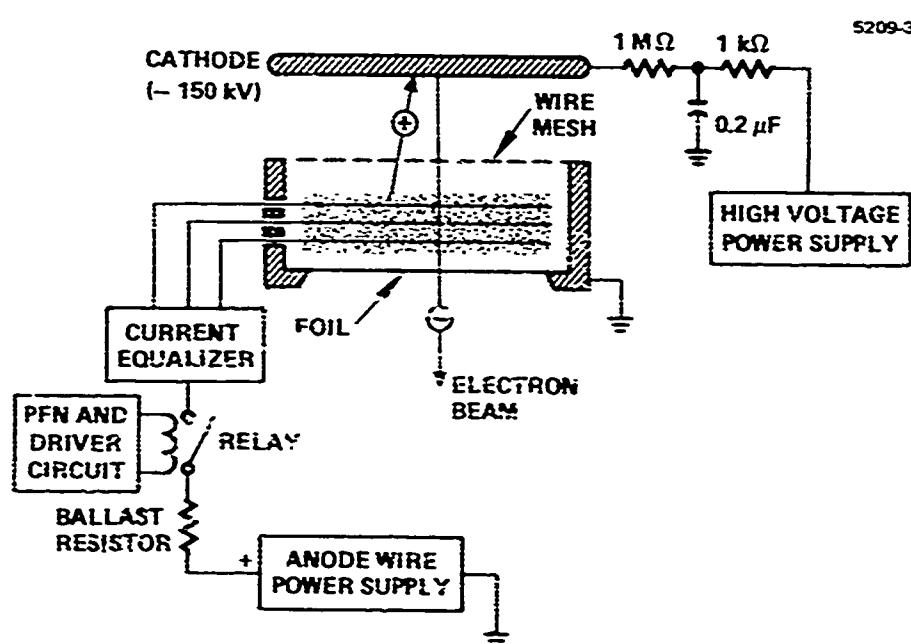
Figure 33.   Ion plasma e-gun test schematic for quasi-
cw operation.

During the experiments the following currents could be monitored with the method described.

1.   Total Cathode Current .

This current, which is the sum of the ion current impinging on and the electron current leaving (due to secondary emission) the cathode, was read using a Pearson current transformer and an oscilloscope readout. The current transformer was placed around a portion of the RG19 high-voltage cable and inside the outer conductor (which connected the high-voltage supply to the gun cathode).

2.   Total Thin-Wire Current

The sum of the currents in the thin-wire discharges was also monitored via a Pearson current transformer.

3.   Faraday Cup Probe Current

For the quasi-dc current measurements, this current was small. To measure the current, the voltage drop across a 10 Ω resistor placed between the cup and ground was read and amplified (gain, 10^3) for display on an oscilloscope. For the short pulsed measurements, in which current levels were much higher, a Pearson current transformer could be used. In both cases the Faraday cup collector was run at +10 V to help eliminate the effects of secondary emission. Even so, the collected current measured in such an arrangement has been estimated to be about 25% less than the actual e-beam current entering the cup aperture.[7] The amplifier display system was carefully calibrated.

4.   Collector Plate Current

Apart from the e-beam current collected by the Faraday cup, this current represents the total transmitted e-beam and was read via a Pearson current transformer in the ground return lead.

C. Experimental Results

Experimental observables and important empirical physical relationships for the ion plasma gun can be classified according to the three regions of the e-gun test apparatus:

- Thin-wire discharge

  Total anode wire current

  Pulse shape

  Pressure dependence of total current and prebreakdown voltage.

- Cathode phenomena

  Voltage and total cathode current

  Relationship of total cathode current to cathode voltage, gas pressure, and pulse width for a given anode wire current.

- Beam Diagnostics

  Extracted e-beam flux, total current, and spatial uniformity.

Extensive efforts were not made to parametrically characterize the thin-wire discharge. From the experiments run, it was found that

- The minimum pressure at which the thin-wire discharge could be initiated was 2 mTorr of helium, as obtained from both thin-wire configurations (Figure 31) and a prebreakdown voltage of 2 kV.

- The pulsed current per unit wire length varied directly with helium gas pressure. The maximum at 20 mTorr pressure was 4.4 A/cm of anode wire length. For the seventeen anode wire configuration (Figure 31(b) and Figure 32), this represented a maximum total anode current of 300 A, which is also the rated current value of the type 5C22 thyratron used.

78

- Variation of series resistance in the thin-
  wire circuit and of charging voltage (i.e.,
  the prebreakdown voltage) also changed the
  peak anode wire current and the pulse width.
  For the tests run, the pulse width was 2 to
  5 usec (FWHM).

The ion plasma e-gun has been operated with a beam voltage as
high as 130 kV, a value limited by the power supply. Most of the data
taken was at a beam voltage of 110 kV. The measured cathode current,
which includes both the incident ion current and the secondary emission
electron current, was monitored as functions of anode wire current and
beam voltage. At a given gas pressure, the total cathode current drawn
(for a given anode current) varied approximately as $V^{3/2}$. As pressure
increased, anode current, cathode current, and the ratio of cathode
current to anode current all increased. There were not sufficient data
taken of this pressure dependence to determine the functional relation-
ship of the variation. Cathode current flux at 110 kV (total cathode
current divided by cathode area) is shown in Figure 34 plotted as a
function of the total anode wire current and in Figure 35 plotted as a
function of the anode current per unit anode wirelength. These data
show that cathode current does not vary linearly with anode current, as
had been predicted by the simple theoretical model presented above. A
least mean square fit of these data yields $J_{cathode} = 0.469 \, I_{\ell 0.789}$ where
$J_{cathode}$ = total cathode current flux (A/cm^2) and I = anode current/
anode wire length (A/cm). This relationship (linear on the log-log plot)
holds very well for over four decades of variation in the currents,
including both the quasi-cw (10 to 150 msec pulse length) and the short
pulse (2 to 5 μsec FWHM) operation. The maximum pulsed cathode
current flux obtained was 2 A/cm^2 at a total anode wire current of 300 A.

Figure 36 shows an oscillogram of the current waveforms for the
total thin-wire anode current and the total cathode current for an 8 msec
pulse length. The droop of the anode wire current waveform is due to
the characteristics of the Pearson Model 2100 current transformer used
for that measurement. Figure 37 shows waveforms for the same two
currents of a 5 μsec FWHM current pulse. Here, the cathode current
has a long (≈40 μsec) fall time. This long fall time has been previously
observed in this kind of gun.[7]

79
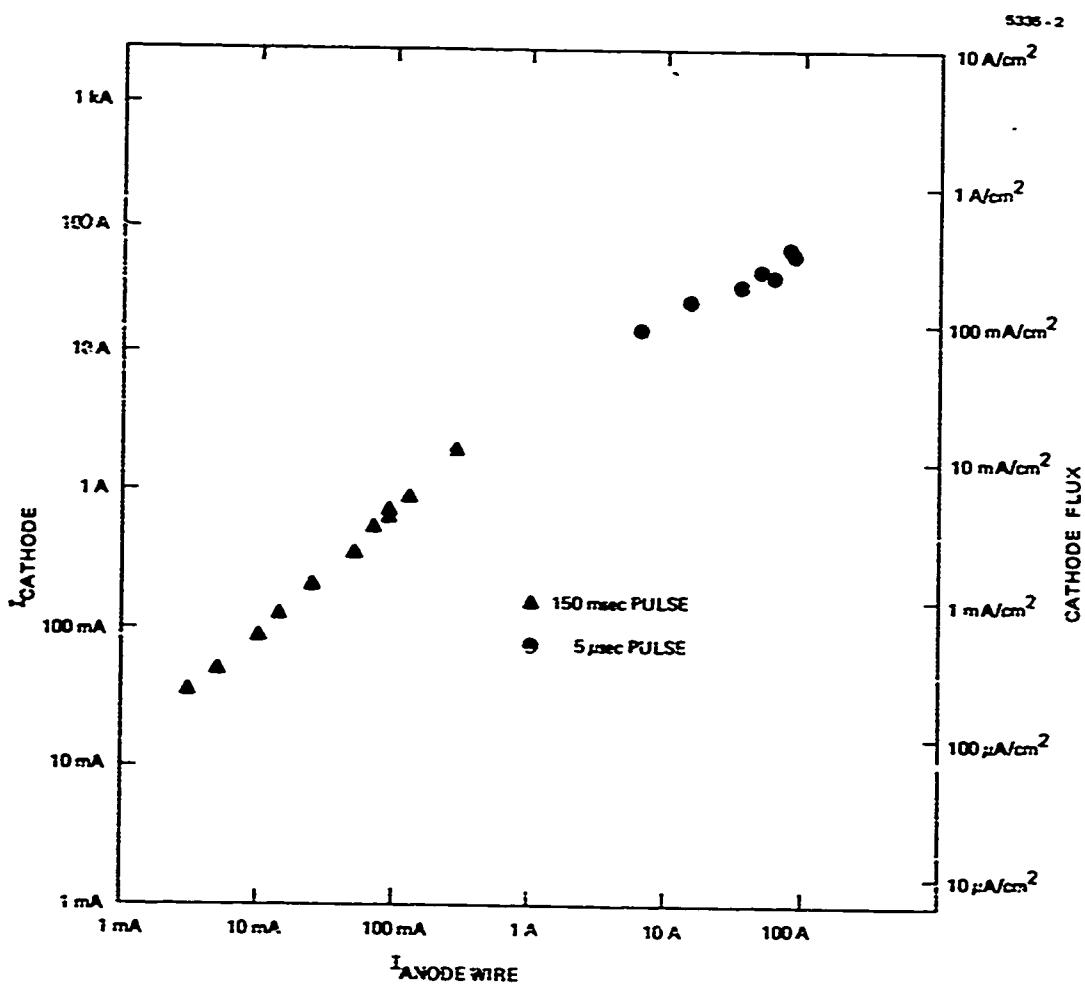
Figure 34. Cathode current output of the ion plasma gun as a function of the anode current input; beam voltage is 110 kV.

80
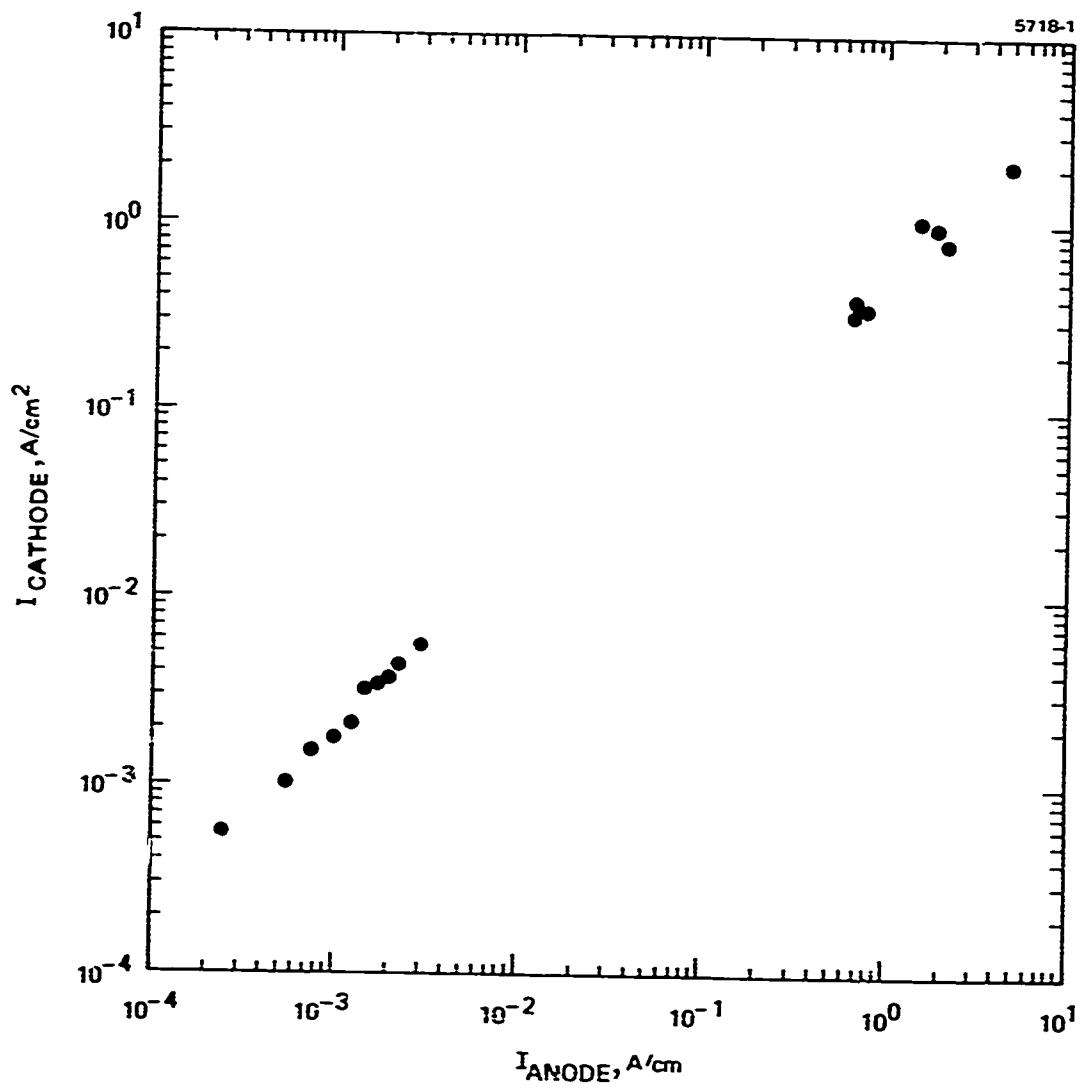
Figure 35. Relationship between the cathode flux and the anode current per unit anode wire length taken for both quasi-cw and short pulse operation at a beam voltage of 110 kV and a gas pressure of 20 mTorr of helium.

81

TOTAL ANODE
WIRE CURRENT
50 mA/div

CATHODE CURRENT
0.5 A/div

SWEEP SPEED
2 msec/div
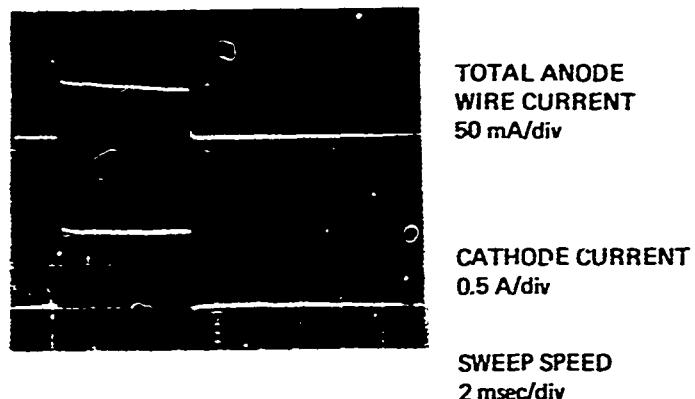
Figure 36.
Anode wire and cathode output current for the
ion plasma e-gun at 110 kV beam voltage and
with quasi-cw (long pulse) operation.

TOTAL ANODE
WIRE CURRENT
100 A/div

CATHODE CURRENT
50 A/div

SWEEP SPEED
1 μsec/div
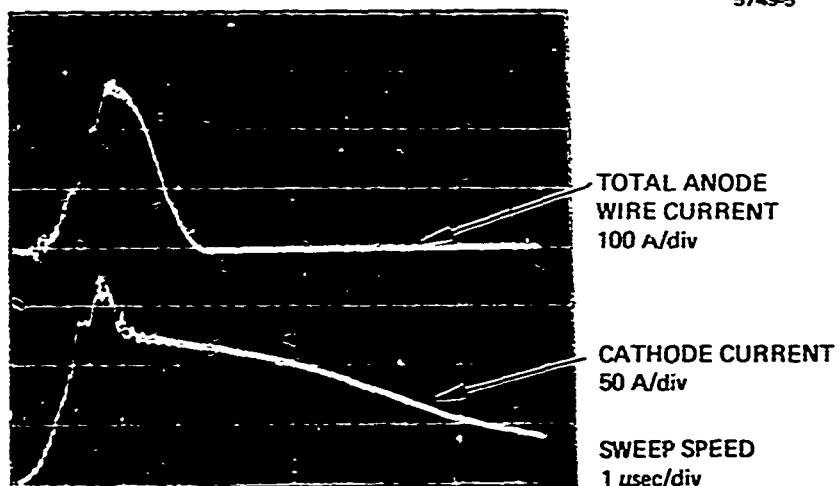
Figure 37.
Anode wire and cathode output current for the ion
plasma e-gun at 110 kV beam voltage with short
pulse operation. Gas pressure 10 mTorr He.

In typical experiments run at a 110 kV beam current, the ratio of the collector plate current to the total cathode current was found to be ≈0.05. Contributing factors were

- The fraction of the total cathode current which was electron current ≈0.91 for a secondary emission coefficient of 10 at the cathode

- Two screen mesh grids, above and below the plasma discharge region, each with a transmission of 0.78 for a total transmission of 0.61

- Foil support transmission of 0.8

- Foil window transmission of ≈0.7

- Reflection of electrons and secondary emission of electrons at the collector plate of ≈0.5

- Shadowing due to the Faraday cup and its support (usually positioned in the center of the beam) of 0.72.

The product of these factors yields a ratio of ~0.11, which is larger than the observed. However, since the collector plate was located 20 cm from the foil, scattering of electrons coming through the foil could have caused them to miss the plate, which could account for the different.

Results on the uniformity of the output current density were taken with the movable Faraday cup for positions along the longitudinal axis of the beam aperture. Two scans of 20 points along the axis were taken at two different values of the cathode current, as shown in Figure 38. For each datum, a separate current pulse of the gun was extracted; the shot-to-shot repeatability of similar pulses with the Faraday cup in a single position was found to be 15%. For the data shown, if account is taken of the ≈15% uncertainty of each point, it may be concluded that the output uniformity of the gun will probably prove to be very good within the central 30 cm of the 40 cm long aperture. Finally, the value of current density read by the Faraday cup probe when positioned in the middle of the aperture was 2 to 3 times larger than the value which would be expected on the basis of the total measured collector plate current. This fact corroborates the earlier

83

statement that secondary emission and reflection at the plate and
scattering of the e-beam from the foil, causing electrons to miss the
plate. accounted for the lower collector plate current readings than
would be expected from other current data.

D.   Discussion and Conclusions

Experiments with the ion plasma electron gun test device were
run over a relatively short time: they were intended to demonstrate the
gun concept and to obtain as large a cathode current as possible. The
emphasis was not on optimizing overall gun performance or on obtain-
ing the data needed to accurately characterize the gun's operation. The
following results were obtained from these experiments:

- **Beam voltage**   Voltage to 130 kV. Higher beam
  voltages were not attempted due to limits on the
  high-voltage power supply. The gun itself
  operated stably with few arcing, corona, or
 other high-voltage breakdown problems.

5391-3
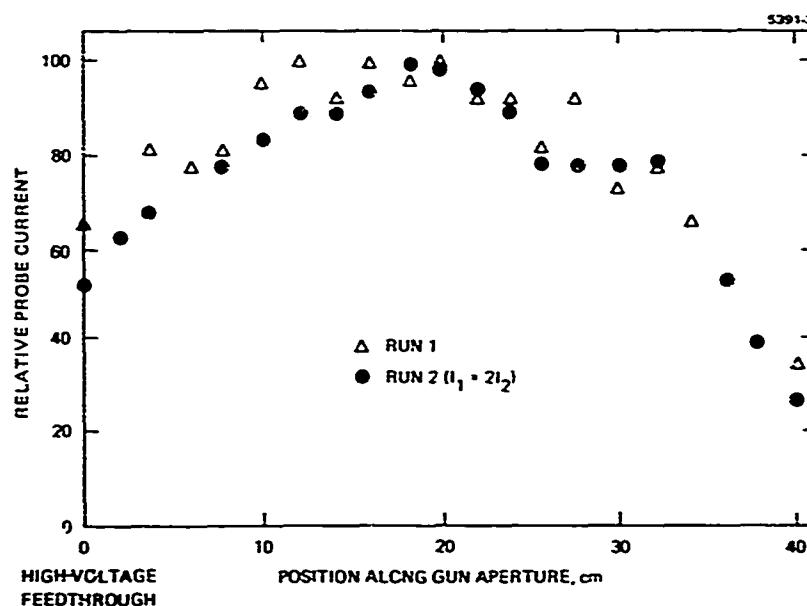
Figure 38.   Uniformity of the output current density
as read by the movable Faraday cup for
8 msec current pulses.

84

- **Pulse length** Length varied from 5 μsec to 150 msec. At the shorter pulse lengths (5 to 10 μsec FWHM), large currents could be drawn from the gun. At long pulse lengths (1 to 150 msec), the gun operated in a cw-type manner in that there were no changes in output characteristics over the entire range of pulse duration except for limitations due to the energy capacity of the power supplies. This fact suggests that these operating times are longer than any transient effects in the gun and that operation is essentially steady state.

- **Output current** A maximum of 320 A cathode current was obtained, which implied a current density of 2 A/cm^2 as limited by existing circuitry. This value of current density was obtained in a 5 μsec pulse length. In the cw-type, long pulse operation, a maximum output current of 2 A (>10 mA/cm^2) was obtained.

- **Pressure** Typical 10 to 20 mTorr of helium. Gun pressure could be lowered to 2 mTorr.

In cw operation, the spatial uniformity of the output current density was measured by means of a moving Faraday cup located downstream of a 0.001 in. thick aluminum foil window. The results of this experiment, based on data for different sets of operating parameters, show that the ion plasma gun gives a beam with good uniformity except for regions just near the edges of the aperture. Within the central portion of the gun aperture, no hot spots or pronounced current minima were observed.

Cathode current was measured at a 110 kV beam voltage for various values of thin-wire anode current, the variation extending over four decades. The results show the relation to be $J_{cathode}$ (A/cm^2) = 0.469 $I_\ell 0.789$, where I_ℓ = anode wire current per unit wire length (A/cm) holds with good accuracy throughout the range of the experiments. This empirical relationship is different from the linear relationship predicted by the simple theoretical model. A more sophisticated theoretical model for the ion plasma e-gun should include the effects of charge exchange and space charge in the acceleration region of the gun. In addition, a detailed model for the thin-wire discharges would be

85

important. In particular, wire length, wire spacing, and system inductance seem to influence the amount of short pulse wire current which can be drawn and the relative amount of cathode current produced.

Space charge effects could limit the current produced by the gun in two ways. The maximum electron current density which can be emitted from the cathode is given by the Child-Langmuir relation $J_e(A/cm^2) = 2.33 \times 10^{-6} (V^{3/2})/d^2$, where d = acceleration gap spacing in centimeters. For the gun used, $d = 4$ cm, which for $V = 110$ kV gives a maximum electron current density of 5.31 A/cm^2. A similar calculation can be made for the maximum ion current extractable from the ion extraction grid; in this calculation, the constant in the Child-Langmuir relation is 2.93×10^{-8} for He^+ ions (to account for the ion mass) and the maximum ion current possible is 0.068 A/cm^2. The secondary emission coefficient of He^+ ions on stainless steel in vacuum is expected to be from 10 to 14; therefore, the maximum electron current obtainable, as limited by space charge on the ions, would be 0.67 to 0.94 A/cm^2, a smaller value than that calculated considering the electron space charge.

As stated above, the maximum cathode current obtained in the experiments was 2 A/cm^2, a value larger than that predicted as the ion space charge limit. In addition, no leveling off of the current transfer relationship was seen, as would be expected if the space charge limit were being approached. To account for the larger than expected cathode current, several explanations may be offered.

> (1) Charge exchange   In this process, helium ions
> in the acceleration region collide with neutral
> helium atoms and exchange electrons, with each
> helium ion creating an energetic neutral (energy
> 200 eV to 110 keV depending on where the
> process takes place in the acceleration region)
> and a slow speed He^+ ion. The energetic neu-
> trals produced have approximately the same
> momentum and energy as the original ion,[13] so
> that these neutrals proceed onto the cathode
> where they produce a comparable number of
> secondary electrons as the ions.[14] Hence the

helium particle flux incident on the cathode
is larger than the ion current by the number
of charge exchange reactions; this leads to
larger observed cathode and secondary elec-
tron currents. Calculations of the charge
exchange mean free path in our system, based
upon published cross-section data,[13] give a
value which is less than 3/4 of the accelerating
gap distance. Charge exchange could account
for the current drawn being 2 to 3 times greater
than would be expected.

(2)   Field-enhanced secondary emission The
secondary emission coefficients reported were
taken from experiments in hich the targets
were in a field-free region. In our case, the
field at the cathode is 5 x 10^4 V/cm, which
could lead to a slight increase in secondary
emission. Such a field is far below the
10^7 V/cm required for field emission and
the effect of microprotrusions to locally
enhance the fields would not appreciably
increase overall current.

(3)   Cathode heating The incident ion flux heats the
cathode surface; a 100°C temperature rise may
be expected if the energy is deposited within
1 μm for a 2 μsec current pulse. This would not
be sufficient for thermionic emission to increase
cathode current significantly.

(4)   Ion space charge neutralization The electron
beam is partially intercepted by the ion extrac-
tion grid, producing slow secondary electrons
in the grid region. Calculations indicate that
7% of the space charge may be neutralized by
this mechanism.

Of the various mechanisms suggested to explain the large cathode cur-
rent, the first, charge exchange, appears the most likely. Detailed
calculations arising from a more sophisticated model of the gun will
will give further insight to these problems. Whatever the mechanisms
at work to produce the current, the maximum current density possible
will be the value calculated from the Child-Langmuir relation for elec-
trons (e. g., 5.3 A/cm^2 for the present gun) which scales as $V^{3/2}/d^2$.

With this scaling, operation of the ion plasma gun with a current density >5 A/cm^2 at 300 kV should be possible.

The advantages of the ion plasma e-gun as a pulsed e-beam pump for high-pressure visible and uv excimer laser systems are

- Longer current pulses than from a cold-cathode field emission gun

- Monoenergetic e-beam, since there is no rise and fall of the high voltage

- DC high voltage for repetitively pulsed operation

- Gun control via relatively low voltages with ground potential based electronics.

Based on the observed performance of the gun, continued development of the ion plasma e-gun to realize these advantages is strongly urged.

IV.   CONCLUSIONS

Two new electron guns were developed on this program for application to e-beam pumped gas lasers. The most effort was directed to the plasma cathode electron gun. In this plasma cathode e-gun, a low-voltage hollow-cathode discharge is the electron source. Recent experiments have demonstrated the attractive features of another new e-gun, the ion plasma electron gun. In this gun, a low-voltage discharge at ground potential produces ions which are accelerated at high voltage; these ions collide with the cathode surface and produce secondary electrons. The secondary electrons are in turn accelerated by the high voltage and extracted as the output electron beam.

The plasma cathode electron gun developed on this program has become a gun which, for cw operation, is a strong competitor to the thermionic e-gun. From this development, large-scale plasma cathode e-guns were built and operated to pump e-beam sustained CO_2 laser systems. Other plasma cathode guns have been used with molecular chemical lasers and to investigate new molecular laser systems. Based on our experience with the guns tested, the plasma cathode gun has the following characteristics.

- **Beam voltage**   Up to 160 kV

- **Beam current density**   Up to 400 $\mu A/cm^2$ (cw) into the foil window for up to 15 min running time. A current density of 1 mA/cm^2 was obtained for shorter time periods; foil heating constraints limit the high-current cw operation.

- **Beam uniformity**   ±5% over the beam aperture except for a fall-off at the ends of the aperture, where the beam density drops over 5 to 8 cm.

- **Gas pressure**   30 to 50 mTorr of helium.

As a result of the progress on this program, two plasma cathode guns were built on other programs to pump e-beam sustained lasers. Both of these guns were designed so that the hollow-cathode beam-extraction area ratio was ≈6 times larger than in the coaxial guns

89

studied in the present program. Both new guns are cw guns and have been operated reliably at helium gas pressures ≤10 mTorr, with a beam current density in excess of 400 $\mu A/cm^2$ (up to 800 $\mu A/cm^2$ for short periods) at 150 kV. One gun, with a 5 cm x 200 cm extracted beam, built at HAC Culver City for the ARPA/Lincoln Labs Laser Radar Power Amplifier, has operated at 150 kV for runs as long as 15 min. Based on all these results, the advantages of the plasma cathode e-gun over a thermionic gun include:

- Simple, rugged construction   No inherently delicate heater elements are required; thermal stress problems are minimized. Smaller size.

- Instantaneous startup   No warmup time. Beam extraction obtained immediately after discharge ignition (which occurs in ≈1 μsec).

- Relative insensitivity to contamination   Foil rupture or leaks do not poison cathode surfaces although purity of the fill gas and vacuum integrity need to be maintained for high-voltage operation.

- High efficiency   The plasma cathode gun consumes less power from supplies floating at high voltages than do equivalent thermionic guns.

- Low cost   Has fewer parts, is simpler, and is easier to scale.

Recent experiments have demonstrated the ion plasma e-gun concept and have shown that this gun has compelling advantages for potential application to repetitively pulsed, high-pressure uv and visible excimer laser systems. The characteristics of this gun as shown by experiments on a gun with a 4 cm x 40 cm beam aperture include:

- Beam voltage   Up to 130 kV (limited by power supply)

- Beam current density   2 A/cm^2 (320 A total) pulsed operation and circuit limited. 12.5 mA/cm^2 (2 A total) for cw operation

- Pulse length   5 μsec FWHM to 150 msec (cw operation also demonstrated)

- **Gas pressure** 2 mTorr to 20 mTorr of helium

- **Beam uniformity** ±10% except for 5 to 8 cm near edge of beam, where current density drops off.

Based on these results, the advantages of the ion plasma electron gun for application to uv and visible excimer laser systems as compared to the cold-cathode field-emission-type e-gun include:

- **Longer current pulses** The ion plasma e-gun does not have a plasma closure constraint on obtaining long current pulses with high current density as does the cold-cathode field-emission gun.

- **Monoenergetic output e-beam** The output energy spread of the beam of the ion plasma gun is determined by the energy spread of the secondary emitted electrons at the cathode surface. This energy spread is estimated to be <40 eV, which represents <0.04% at 110 kV beam voltage. There are no low-energy electrons emitted due to the rise and fall of the gun voltage as present with Marx-bank-driven field emission guns.

- **DC high voltage** This makes application for repetitively pulsed lasers much simpler.

- **Gun control at ground potential** The gun is controlled by switching on the thin-wire discharges (≤2 kV) with electronics located at ground potential. Neither high-voltage switching (Marx bank) nor electronics floating at high voltage (thermionic guns) is required.

Based on a theoretical model developed for the gun, estimates can be made of the scaling of both current density and beam voltage. Beam voltage constraints are primarily determined by Paschen breakdown at the helium gas pressure used (2 to 10 mTorr for high-voltage vacuum breakdown limits). From these considerations it can reasonably be expected that it is possible to design and operate an ion plasma e-gun with a beam voltage >400 kV. Current density should scale as $V^{3/2}/d^2$ (d = gap spacing). This scaling appears true experimentally,

based on a limited amount of data, and would indicate that a 400 keV beam at 5 to 10 A/cm^2 density should be obtainable. The maximum current density will be determined by space-charge constraints on the ions and electrons present within the accelerating gap of the gun.

REFERENCES

1.   H. Helm, "Experimenteller Nachweis des Pendel — Effektes in Ciner Zylindrischen Niederdruck — Hohlkathoden — Entlandung in Argon," Z_o fur Naturforshung $\underline{27A}$, 1812-1820 (1972).

2.   W. Lotz, "An Empirical Formula for the Electron-Impact Ionization Cross-Section," Z. fur Physik $\underline{206}$, 250-211 (1967).

3.   W.H. K , Handbook of Materials and Techniques for Vacuum Devices (Reinhold Publishing Corp., New York, 1967), pp. 588-596.

4.   L.G. Guseva, Sov. Phys.-Tech. Phys. $\underline{15}$, 1760 (1971).
      D.D. Aleksandrov, N.F. Olendzkaia, and S.V. Ptitsyn, Sov.
5.   Phys.-Tec.Phys. $\underline{3}$, 836 (1958).

5.   M.J. Schonhuber, "Breakdown of Gases Below Paschen Minimum," IEEE Trans. on Power Apparatus and Systems $\underline{88}$, 100 (1969).

6.   K. Spangenberg, Vacuum Tubes (McGraw-Hill, New York, 1948), pp. 125-161.

7.   D. Pigache and G. Fournier, "Secondary Emission Electron Gun for High Pressure Molecular Lasers," J. Vac. Sci. Technol. $\underline{12}$, 1197-1199, Nov./Dec. 1975.

8.   G. Wakalopulos, "Ion Plasma Electron Gun," U.S. Patent No. 3,970,892, Hughes Aircraft Co., Culver City, Calif. July 20, 1976.

9.   G.W. McClure, "Low Pressure Glow Discharge," Appl. Phys. Lett. $\underline{2}$, 233-234 June 1963.

10.   G.W. McClure, "High Voltage Glow Discharges in D_2 Gas. I. Diagnostic Measurements," Phys. Rev. 124 969-982, Nov. 1961.

11.   A.G. Hill et al., "The Emission of Secondary Electrons Under High Energy Positive Ion Bombardment " Phys. Rev. $\underline{55}$, 463-470, March 1939.

12.   G. Carter and J. Colligon, Ion Bombardment of Solids (Heineman Educational Books Ltd., London 1968), Ch. 3.

13.   S. Allison, "Experimental Results on Charge-Changing Collisions of Hydrogen and Helium Atoms and Ions at Kinetic Energies above 0.2 keV," Rev. Mod. Phys. $\underline{30}$, 1137 (1958).

14.   F. Schwarzke, "Ionisterungs-und Umiadequerschnitte von Wasserstoff-Atomen und Ionen von 9 bis 60 keV in Wasserstaff," Zeitsch, fur physik $\underline{157}$, 510-522 (1960).